THE JOURNAL OF BIOLOGICAL CHEMISTRY VOL. 292, NO. 9, pp. 3552–3567, March 3, 2017

A Quininib Analogue and Cysteinyl Leukotriene Receptor Antagonist Inhibits Vascular Endothelial Growth Factor (VEGF)-independent Angiogenesis and Exerts an Additive Antiangiogenic Response with Bevacizumab*

Received for publication, July 27, 2016, and in revised form, December 19, 2016 Published, JBC Papers in Press, December 29, 2016, DOI 10.1074/jbc.M116.747766

Clare T. Butler[‡], Alison L. Reynolds[‡], Miriam Tosetto[§], Eugene T. Dillon[‡], Patrick J. Guiry[¶], Gerard Cagney[‡], Jacintha O'Sullivan[‖], and Breandán N. Kennedy[‡1]

From the [‡]UCD School of Biomolecular and Biomedical Science, UCD Conway Institute and [¶]UCD School of Chemistry, UCD Centre for Synthesis and Chemical Biology, University College Dublin, Belfield, Dublin 4, Ireland, [§]Centre for Colorectal Disease, St. Vincent's University Hospital, Dublin 4, Ireland, and [‖]Trinity Translational Medicine Institute, Department of Surgery, Trinity College Dublin, St. James's Hospital, Dublin 8, Ireland

Edited by Henrik G. Dohlman

Excess blood vessel growth contributes to the pathology of metastatic cancers and age-related retinopathies. Despite development of improved treatments, these conditions are associated with high economic costs and drug resistance. Bevacizumab (Avastin®), a monoclonal antibody against vascular endothelial growth factor (VEGF), is used clinically to treat certain types of metastatic cancers. Unfortunately, many patients do not respond or inevitably become resistant to bevacizumab, highlighting the need for more effective antiangiogenic drugs with novel mechanisms of action. Previous studies discovered quininib, an antiangiogenic small molecule antagonist of cysteinyl leukotriene receptors 1 and 2 ($CysLT_1$ and $CysLT_2$). Here, we screened a series of quininib analogues and identified a more potent antiangiogenic novel chemical entity (IUPAC name (*E*)-2-(2-quinolin-2-yl-vinyl)-benzene-1,4-diol HCl) hereafter designated Q8. Q8 inhibits developmental angiogenesis in Tg(*fli1*:EGFP) zebrafish and inhibits human microvascular endothelial cell (HMEC-1) proliferation, tubule formation, and migration. Q8 elicits antiangiogenic effects in a VEGF-independent *in vitro* model of angiogenesis and exerts an additive antiangiogenic response with the anti-VEGF biologic bevacizumab. Cell-based receptor binding assays confirm that Q8 is a $CysLT_1$ antagonist and is sufficient to reduce cellular levels of NF-κB and calpain-2 and secreted levels of the proangiogenic proteins intercellular adhesion molecule-1, vascular cell adhesion protein-1, and VEGF. Distinct reductions of VEGF by bevacizumab explain the additive antiangiogenic effects observed in combination with Q8. In summary, Q8 is a more effective antiangiogenic drug compared with quininib. The VEGF-independent activity coupled with the additive antiangiogenic response observed in combination with bevacizumab demonstrates that Q8 offers an alternative therapeutic strategy to combat resistance associated with conventional anti-VEGF therapies.

Angiogenesis is a highly regulated physiological process in health and disease that enables the formation of new blood vessels (1). Enhanced angiogenesis occurs pathologically in response to hypoxia and inflammation in disorders such as cancer, psoriasis, blindness, diabetes, and arthritis (2), impacting the health of millions of people worldwide (2–5).

Angiogenesis is regulated by a balance of pro- and antiangiogenic factors and arises from a stepwise process wherein endothelial cells dissociate from pericyte cells and their basement membrane, moving toward the target tissue requiring vascularization (6, 7). Secreted factors can enhance or inhibit this process. Inducers of this process include vascular endothelial growth factors (VEGFs), angiopoietins, transforming growth factors (TGFs), platelet-derived growth factors (PDGFs), tumor necrosis factor-α (TNF-α), interleukins, and fibroblast growth factor (FGF) proteins (8). Angiogenesis is also regulated by membrane bound proteins including vascular cell adhesion molecule-1 (VCAM-1)[2] and intercellular adhesion molecule-1 (ICAM-1), which enable cell-matrix or cell-cell interactions (9–11). Angiogenesis is a frequently targeted process in the discovery of new drugs for cancer and blindness. Annual costs of cancer treatment and care are estimated to escalate to $173,000,000 in 2020, and the majority of new therapies cost ~$5,000 per month (12, 13). Unfortunately, these expensive therapies often exert limited overall therapeutic benefit (14).

Bevacizumab (Avastin®), a monoclonal antibody against soluble VEGF, restricts the progression of tumor angiogenesis (15) and choroidal neovascularization (16) by preventing VEGF

* This work was supported by Irish Cancer Society Scholarship Grant CRS13BUT and Enterprise Ireland Grant CF/20111319. J. O. and B. N. K. are inventors on United States Patent 8916586 B2, and A. L. R., J. O., and B. N. K. are inventors on United States Patent 9388138 B2.

[1] To whom correspondence should be addressed: F062 UCD Conway Institute, UCD School of Biomolecular and Biomedical Science, UCD Conway Institute, University College Dublin, Belfield, Dublin D04 V1W8, Ireland. Tel.: 353-1-716-6740; E-mail: brendan.kennedy@ucd.ie.

[2] The abbreviations used are: VCAM-1, vascular cell adhesion molecule-1; ICAM-1, intercellular adhesion molecule-1; $CysLT_1$, cysteinyl leukotriene receptor-1; HMEC-1, human microvascular endothelial cells-1; LT, leukotriene; Q1, quininib (2-[(*E*)-2-(quinolin-2-yl)vinyl]phenol); Q8, (*E*)-2-(2-quinolin-2-yl-vinyl)-benzene-1,4-diol HCl; Q7, (*E*)-2-(2-quinolin-2-yl-vinyl)-benzene-1,4-diol; Q18, (*Z*)-2-(2-(quinolin-2-yl)vinyl)phenol HCl; Q22, 2-quinolin-2-yl-ylethynylphenol; ISV, intersegmental vessel; dpf, day(s) postfertilization; hpf, hours postfertilization; CIM, cell invasion/migration; RTCA, real time cell analyzer; PI, propidium iodide; VEGFR, vascular endothelial growth factor receptor; bFGF, basic fibroblast growth factor; MTT, 3-(4,5-dimethylthiazol-2-yl)-2,5-diphenyltetrazolium bromide; KDR, kinase insert domain receptor; EGFP, enhanced green fluorescent protein; ANOVA, analysis of variance; Ang, angiopoietin.

from interacting with vascular endothelial growth factor receptor-2 (VEGFR2). However, a combination of this anti-VEGF biologic with chemotherapy has limited therapeutic effects, merely prolonging the survival of metastatic colorectal cancer patients by ~4.7 months (17) and lung cancer patients by ~13 months (18) and increasing progression-free survival of breast cancer patients by ~2–25 months (19, 20). The clinical efficacy of bevacizumab is only apparent in combination with chemotherapy as it can stabilize leaky tumor vessels, enhancing delivery of chemotherapy to the tumor. There is an unmet clinical need for the development of more effective treatments that have the ability to inhibit alternative regulators of angiogenesis, overcoming treatment resistance to antiangiogenic therapy. New drug discovery is impeded by the small number of novel and validated disease targets (21). Target-based drug discovery focuses on specific known protein targets and overlooks the possible importance of less well functionally understood proteins that may be involved in disease mechanism. Hence, phenotype-based drug screening is re-emerging as an effective means of moving beyond well understood targets to discover novel drug targets and understand the physiology and pathophysiology of disease (21).

Previous phenotype-based chemical screens discovered quininib (2-[(*E*)-2-(quinolin-2-yl)vinyl]phenol), a small quinoline molecule with novel antiangiogenic activity (22–24). Quininib antagonizes cysteinyl leukotriene receptors 1 and 2 ($CysLT_1$ and $CysLT_2$), does not target VEGF receptors, and inhibits phosphorylated ERK, a $CysLT_1$ downstream effector (22). Cysteinyl leukotrienes LTC_4, LTD_4, and LTE_4 are lipid mediators produced from arachidonic acid via the 5-lipoxygenase pathway (25). They are agonists for the G-protein-coupled cysteinyl leukotriene receptors $CysLT_1$ and $CysLT_2$ and the less functionally studied GPR17 and GPR99 ($CysLT_3$) (26).

CysLT receptors are aberrantly expressed in tumors; enhanced expression of $CysLT_1$ in colorectal cancer negatively correlates with patient survival (27), and antagonism of $CysLT_1$ significantly reduces angiogenesis in rodent models (28). Collectively, this reveals an important biological role for CysLT signaling during neovascular disease and an alternative therapeutic target.

Here, 24 structurally distinct analogues of quininib were ranked. Analogues Q22 (IUPAC name 2-quinolin-2-yl-ylethynylphenol), Q18 (IUPAC name (*Z*)-2-(2-(quinolin-2-yl)vinyl) phenol HCl), and Q8 (IUPAC name (*E*)-2-(2-quinolin-2-yl-vinyl)-benzene-1,4-diol HCl) were significantly more effective than quininib at inhibiting angiogenesis *in vivo* with Q8 being the most potent analogue. Q8 inhibits human endothelial cell tubule formation and migration. Ligand binding assays confirm that Q8 is also a $CysLT_1$ antagonist. Further to what we previously reported regarding the mechanism of action of quininib (22), the structurally distinct Q8 analogue significantly reduces cellular levels of proangiogenic signals NF-κB and calpain-2 and secreted levels of ICAM-1, VCAM-1, and VEGF compared with quininib. Additionally, Q8 inhibits *in vitro* models of angiogenesis that do not rely on endogenous VEGF and exerts an additive antiangiogenic effect with bevacizumab.

Results

Analogues Have Enhanced Antiangiogenic Effects in Vivo Compared with Quininib (Q1)—The small molecule Q1 was previously identified to inhibit ocular angiogenesis in the zebrafish hyaloid vascular assay and tumor angiogenesis (22–24). Here, we sought to identify novel chemical entities with more potent antiangiogenic effects *in vivo* using the zebrafish intersegmental vessel assay. Preliminary analyses of 37 structural quininib analogues identified drugs that robustly inhibited developmental angiogenesis in larval zebrafish eyes (29). In these analogues, the position of the phenyl ring hydroxy group and/or the linkage between the quinoline and phenyl ring was modified (Fig. 1*A*). Initially, we ranked the bioactivity of 24 salt or amine analogue formulations by comparing the ability of a 10 μM concentration of the drugs to inhibit developmental angiogenesis in the intersegmental vessel (ISV) assay using Tg(*fli1*:EGFP) zebrafish (Fig. 1, *B* and *C*). Twelve analogue formulations produced a statistically significant inhibition of developmental angiogenesis compared with control (Fig. 1*C*). Of these, one analogue, Q22, produced antiangiogenic activity equivalent to quininib, and two analogues, Q8 and Q18, produced a greater antiangiogenic activity compared with quininib at 10 μM ($p < 0.05$) (Fig. 1*C*). Q22 includes an alkyne linkage between the quinoline and phenyl ring, whereas Q18 is the *Z*-enantiomer of quininib. Notably, Q7 (IUPAC name (*E*)-2-(2-quinolin-2-yl-vinyl)-benzene-1,4-diol) in amine and hydrochloride salt forms (Q8) was toxic to larvae at 10 μM. Q7 and Q8 include two hydroxy groups in the phenyl ring at positions R_1 and R_4. Quininib, Q18, Q22, and Q8 were rescreened in the ISV assay at concentrations increasing from 0.1 to 10 μM (Fig. 1, *D* and *E*). All novel analogues tested resulted in a dose-dependent inhibition of ISV development. Interestingly, only Q8 and Q18 were significantly bioactive at 1 μM, reducing ISV development compared with control by 75 and 30%, respectively (Fig. 1*E*). Q8 reduced ISV development more potently than any other analogue tested and was the only analogue significantly active at 0.5 μM, inhibiting developmental angiogenesis by 12.4%. All analogues produced varying degrees of pericardial edema at 2 days postfertilization (dpf). No other adverse morphological defects were detected following treatment with the analogues at 2 dpf (Fig. 1*D*). In summary, using an analogue ranking system based on maximum inhibition of ISV development and potency, Q8 was identified as the most effective quininib analogue (Table 1).

Quininib Analogues Reduce Endothelial Cell Number after 24 h and Inhibit Endothelial Cell Migration—Quininib and the highest ranking analogues were tested for effects on cell number in human microvascular endothelial cells (HMEC-1) following 24-, 72-, and 96-h treatment (Fig. 2*A*). 10 μM quininib and analogues had no effect on HMEC-1 cell number compared with control at 24 h. However, at 72 h, 5-fluorouracil, Q8, and Q18 significantly reduced endothelial cell number compared with vehicle control ($p > 0.001$). After 96 h of treatment, all compounds reduced cell number significantly compared with 0.1% DMSO control.

Using a CIM plate 16 xCELLigence® RTCA platform (Roche Applied Science), the migratory behavior of drug-treated HMEC-1 endothelial cells was quantified over 8 h (Fig. 2*A*). All

A. Structures of quininib analogues

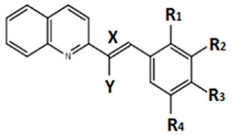

Compound	IUPAC name	X	Y	R_1	R_2	R_3	R_4	Salt
Q1-Quininib	2-[(*E*)-2-Quinolin-2-yl)vinyl]phenol	Alkene	-	OH	-	-	-	-
Q2	2-[(*E*)-2-Quinolin-2-yl)vinyl]phenol HCl salt	Alkene	-	OH	-	-	-	HCl
Q3	3-(2-Quinolin-2-yl-vinyl)-phenol	Alkene	-	-	OH	-	-	-
Q4	3-(2-Quinolin-2-yl-vinyl)-phenol HCl salt	Alkene	-	-	OH	-	-	HCl
Q5	4-(2-Quinolin-2-yl-vinyl)-phenol	Alkene	-	-	-	OH	-	-
Q6	4-(2-Quinolin-2-yl-vinyl)-phenol HCl salt	Alkene	-	-	-	OH	-	HCl
Q7	(E)-2-(2-Quinolin-2-yl-vinyl)- -benzene-1,4-diol	Alkene	-	OH	-	-	OH	-
Q8	(E)-2-(2-Quinolin-2-yl-vinyl)- -benzene-1,4-diol HCl salt	Alkene	-	OH	-	-	OH	HCl
Q9	(E)-2-(2-Quinolin-2-yl-vinyl)- -benzene-2,4-diol	Alkene	-	-	OH	-	OH	-
Q10	(E)-2-(2-Quinolin-2-yl-vinyl)-benzene-2,4-diol HCl salt	Alkene	-	-	OH	-	OH	HCl
Q11	2-(2-Quinolin-2-yl-ethyl)-phenol	Alkane	-	OH	-	-	-	-
Q12	2-(2-Quinolin-2-yl-ethyl)-phenol HCl salt	Alkane	-	OH	-	-	-	HCl
Q13	3-(2-Quinolin-2-yl-ethyl)-phenol	Alkane	-	-	OH	-	-	-
Q14	3-(2-Quinolin-2-yl-ethyl)-phenol HCl salt	Alkane	-	-	OH	-	-	HCl
Q15	4-(2-Quinolin-2-yl-ethyl)-phenol	Alkane	-	-	-	OH	-	-
Q16	4-(2-Quinolin-2-yl-ethyl)-phenol HCl salt	Alkane	-	-	-	OH	-	HCl
Q17	(Z)-2-(2-(Quinolin-2-yl)vinyl) phenol	Z-Alkene	-	OH	-	-	-	-
Q18	(Z)-2-(2-(Quinolin-2-yl)vinyl) phenol HCl salt	Z-Alkene	-	OH	-	-	-	HCl
Q19	(E)-2-(2-Quinolin-2-yl-propenyl)-phenol	Alkene	Me	OH	-	-	-	-
Q20	(E)-2-(2-Quinolin-2-yl-propenyl)-phenol HCl salt	Alkene	Me	OH	-	-	-	HCl
Q21	2-Quinolin-2-yl-ylethynyl-phenol	Alkyne	-	OH	-	-	-	-
Q22	2-Quinolin-2-yl-ylethynyl-phenol HCl salt	Alkyne	-	OH	-	-	-	HCl
Q23	3-Quinolin-2-yl-ylethynyl-phenol	Alkyne	-	-	OH	-	-	-
Q24	3-Quinolin-2-yl-ylethynyl-phenol HCl salt	Alkyne	-	-	OH	-	-	HCl
Q25	4-Quinolin-2-yl-ylethynyl-phenol	Alkyne	-	-	-	OH	-	-
Q26	4-Quinolin-2-yl-ylethynyl-phenol HCl salt	Alkyne	-	-	-	OH	-	HCl

B. ISV assay

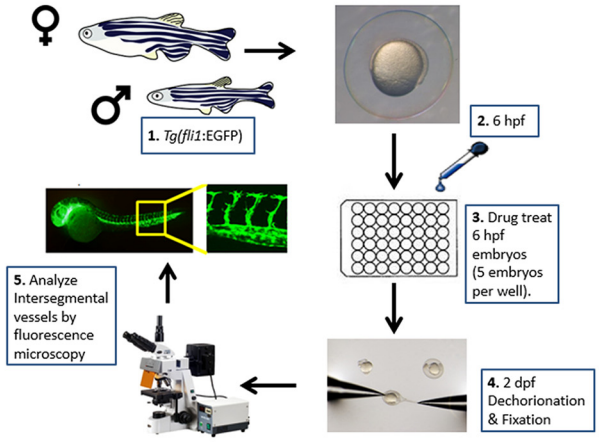

C. ISV screening of quininib analogues

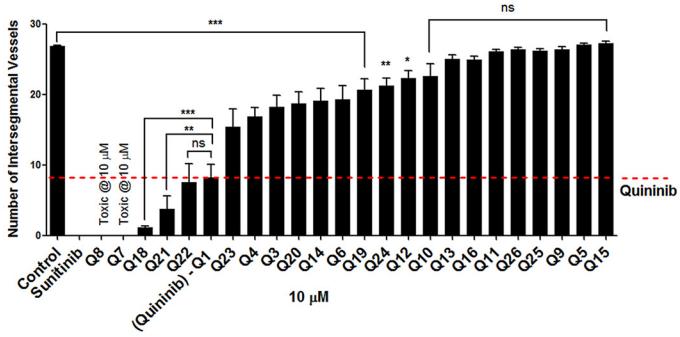

D. ISV images - analogue treated larvae (2dpf)

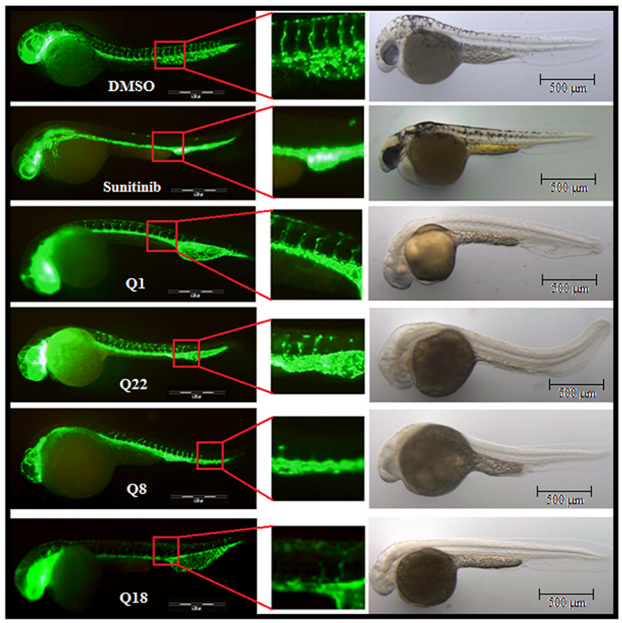

E. ISV dose response highest ranking analogue salts

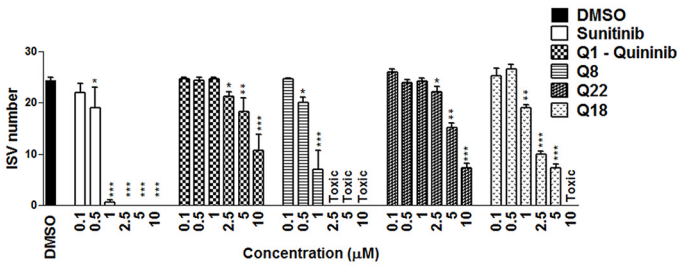

FIGURE 1. **Analogues more effectively inhibit developmental angiogenesis compared with quininib *in vivo*.** *A*, structural skeleton of the quininib drug series and table listing the differences in chemical structures of all quininib analogues. A synthesis scheme for each chemical is included in Kennedy *et al.* (29). *B*, schematic of the intersegmental vessel assay. Male and female Tg(*fli1*:EGFP) zebrafish were in-crossed, yielding embryos that were treated with quininib analogues at 6 hpf. Larvae were dechorionated and fixed at 2 dpf, and intersegmental vessels were counted by visualizing under fluorescence microscopy. *C*, ranking graph of the bioactivity of 24 salt or amine analogue formulations comparing the ability of a 10 μM concentration of each analogue to inhibit developmental angiogenesis in the ISV assay using Tg(*fli1*:EGFP) zebrafish. *D*, fluorescence images of Tg(*fli1*:EGFP) treated with the most effective concentrations of analogues (0.1% DMSO, 10 μM sunitinib, 10 μM Q1, 10 μM Q22, 1 μM Q8, and 5 μM Q18). *E*, dose-response graph following rescreening of quininib analogues in the ISV assay at concentrations increasing from 0.1 to 10 μM. Individual experiments consisted of treating five embryos per well in duplicate (10 embryos), and individual experiments were conducted three times ($n = 3$). Statistical analysis was performed by ANOVA and Dunnett's or Bonferroni's post hoc multiple comparison test. *Error bars* are mean ± S.E. *, $p < 0.05$; **, $p < 0.01$; ***, $p < 0.001$; *ns*, not significant.

analogues except Q1 significantly inhibited HMEC-1 endothelial cell migration with Q8 producing the most significant effect, inhibiting endothelial migration by ~79% ($p < 0.001$) (Fig. 2*B*). We also investigated whether a combination of either 1 or 3 μM Q8 with bevacizumab had additive effects on HMEC-1 endothelial cell migration (Fig. 2*C*). Compared with control, treatments with 2.5 μg/μl bevacizumab, 1 or 3 μM Q8, or 2.5 μg/μl bevacizumab in combination with 1 μM Q8 did not significantly reduce HMEC-1 migration. However, 2.5 μg/μl bevacizumab in combination with 3 μM Q8 significantly reduced migration compared with control ($p < 0.046$) and with 2.5 μg/μl bevacizumab ($p < 0.039$) but not with 3 μM Q8 alone

TABLE 1
Analogue ISV dose response and ranking based on efficacy, potency, and toxicity

Compound	IUPAC name	Efficacy score	Potency score	Toxicity score	Total score	Rank
Q8	(*E*)-2-(2-Quinolin-2-yl-vinyl)-benzene-1,4-diol HCl salt	4	5	4	13	1[a]
Q18	(*Z*)-2-(2-(Quinolin-2-yl)vinyl)phenol HCl salt	4	4	4	12	2
Q22	2-Quinolin-2-yl-ylethynylphenol HCl salt	4	3	4	11	3
Q1	2-[(*E*)-2-(Quinolin-2-yl)vinyl]phenol	3	3	4	10	4

[a] Highest ranking compound in ISV assay based on efficacy and potency scoring system.

($p < 0.2615$). As observed with previous migration analyses, 10 μM Q8 induced the most statistically significant reduction of HMEC-1 cell migration compared with control ($p < 0.002$).

In summary, Q8 and Q18 significantly reduced HMEC-1 endothelial cell number at 72 and 96 h, whereas Q1 and Q22 showed significant reductions in cell number at 96 h only. Analogues of quininib, particularly Q8, impede endothelial cell migration, a surrogate measure of angiogenesis.

Quininib Analogues Inhibit Human Endothelial Cell Tubule Formation and Do Not Affect HMEC-1 Viability—Previous studies demonstrated that 10 μM Q1 had modest effects on endothelial tubule formation in human dermal microvascular endothelial cells (23). Here, we tested the dose-dependent effects of Q1 and its analogues (Q8, Q18, and Q22) on HMEC-1 tubule formation using μ-Slide angiogenesis plates (ibidi GmbH). Q1 significantly inhibited tubule formation at 3 and 10 μM but not at 1 μM (Fig. 3*A*). Following 16-h treatment, Q8 and Q18 were significantly more effective than quininib at inhibiting HMEC-1 tubule formation at all concentrations tested (1–10 μM) ($p < 0.01$). Q8 and Q18 were the most effective compounds, inhibiting tubule formation at 10 μM by ~98 and 78%, respectively ($p < 0.05$). Potential cytotoxic effects of analogue Q8 were ruled out by co-staining HMEC-1 endothelial cell tubules with calcein and propidium iodide (PI) following 16-h exposure (Fig. 3*C*). No concentrations of Q8 tested (0.1–20 μM) induced any significant endothelial cell death as shown by a lack of PI staining (*red*) compared with cells treated with 10 μM sunitinib, which stained positively for PI (Fig. 3*C*). In addition, calcein (*green*) was taken up by the cells treated with all concentrations of Q8, indicating that HMEC-1 cells are viable following 16-h treatment with the Q8 analogue.

Quininib Analogues Inhibit VEGF-independent Angiogenesis in Vitro—We investigated the effects of the clinically used VEGF-neutralizing antibody bevacizumab on tubule formation by incubating HMEC-1 cells with varying concentrations of bevacizumab ranging from 2.5 to 10 μg/μl, all of which had no effect on tubule formation compared with control or IgG isotype control (Fig. 4, *A* and *B*). Furthermore, higher concentrations of bevacizumab (5 and 10 μg/μl) did not significantly affect HMEC-1 tubule formation (data not shown). The addition of 10 ng/ml recombinant VEGF increased endothelial cell tubule formation by ~20% compared with control ($p = 0.0082$). Following addition of both 2.5 μg/μl bevacizumab and 10 ng/ml VEGF, tubule formation was significantly decreased by ~45% compared with 10 ng/ml VEGF alone ($p < 0.05$) (Fig. 4, *A* and *B*). We conclude that our HMEC-1 *in vitro* tubule formation assays are not dependent on basal VEGF, but exogenous VEGF is sufficient to induce enhanced tubule formation. We examined the effects on tubule formation when treating cells with quininib or Q8 in the presence of exogenous VEGF. Interestingly, ectopic VEGF could suppress the antiangiogenic effects of quininib drugs but not the anti-VEGF biologic, supporting distinct mechanisms of action of these antiangiogenic drugs. In the presence of exogenous VEGF, quininib or Q8 produced a more modest inhibition of tubule formation compared with treatment with either drug alone (Fig. 4, *C* and *D*). In summary, the quininib small molecule drugs are efficacious at inhibiting a VEGF-independent model of *in vitro* angiogenesis. The VEGF-independent antiangiogenic action of these drugs is further supported by a lowered antiangiogenic activity in the presence of recombinant VEGF.

Q8 Has Additive Antiangiogenic Effects with an Anti-VEGF Biologic, Bevacizumab—The distinct mechanisms of action inferred above led us to investigate the *in vitro* antiangiogenic effects of our lead small molecule drug Q8 in combination with bevacizumab. HMEC-1 endothelial cells were treated with a combination of either 3 μM Q1 and 2.5 μg/μl bevacizumab or 1 μM Q8 and 2.5 μg/μl bevacizumab (Fig. 5, *A* and *B*). Concentrations of Q1 (3 μM) and Q8 (1 μM) producing equivalent ($p = 0.1163$) (~45–65%) intermediate responses were selected for the combination study (Fig. 3*A*). As bevacizumab requires the presence of exogenous VEGF to bring about an antiangiogenic effect (Fig. 4*A*), combination treatment groups were supplemented with 10 ng/ml recombinant VEGF. Compared with either Q8 or bevacizumab treatment alone, treatment of HMEC-1 cells with the combination of Q8 and bevacizumab induced an additive significant reduction in tubule formation ($p = 0.0174$) (Fig. 5, *A* and *B*). This additive effect was observed with Q8 and not with Q1 (Fig. 5, *A* and *B*). There was no statistically significant difference in tubule formation observed between Q8-alone and bevacizumab-alone treatment groups. In addition, an isotype control that consisted of a combination of 1 μM Q8 and 2.5 μg/μl IgG did not alter tubule formation compared with Q8 or bevacizumab alone. However, compared with the isotype control combination treatment, 1 μM Q8 and 2.5 μg/μl bevacizumab combination treatment significantly reduced tubule formation, signifying the specificity of bevacizumab in the antiangiogenic combination effect. In conclusion, specific, enhanced antiangiogenic effects are demonstrated following treatment of human endothelial cells with a combination of both Q8 and an anti-VEGF biologic, bevacizumab.

Quininib Analogue Q8 Is a Cysteinyl Leukotriene Receptor-1 Antagonist and Regulates Inflammatory and Angiogenic Signaling Pathways—The $CysLT_1$ receptor was previously identified as a quininib target (22). Here, we determined the IC_{50} of Q8 for $CysLT_1$ receptor to be 4.9 μM in a CHO cell-based receptor antagonism assay. The highest concentration of Q8 tested (50 μM) inhibited $CysLT_1$ activation by 113% (Fig. 6*A*). In contrast,

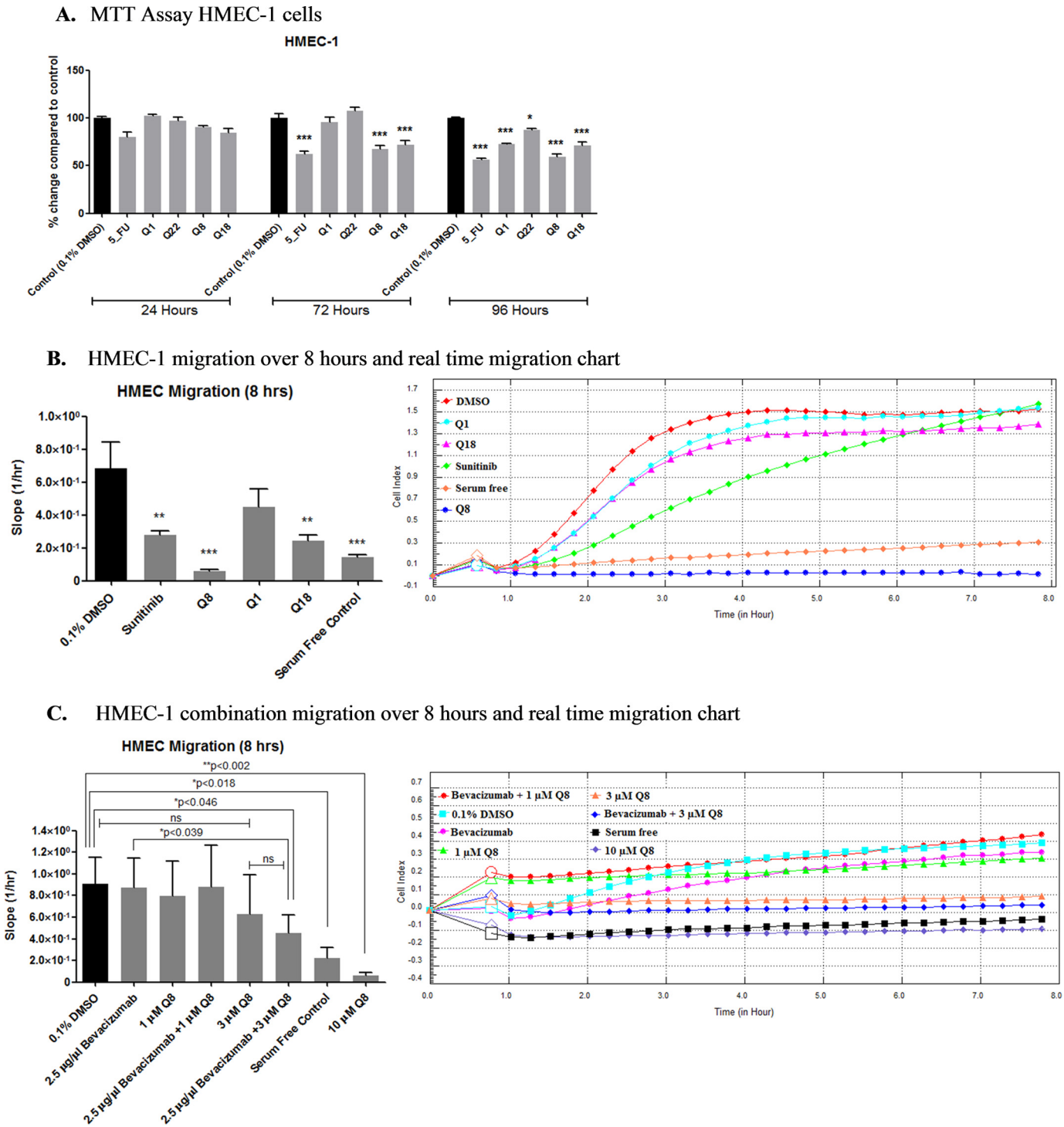

FIGURE 2. **Quininib analogues reduce endothelial cell number after 24 h and inhibit endothelial cell migration.** *A*, effect of 10 μM quininib analogues on HMEC-1 endothelial cell number using the MTT assay following 24-, 72-, and 96-h treatment. 10,000 cells were seeded and treated in duplicate for each individual experiment, and individual experiments were conducted three times ($n = 3$). *B*, effect of 10 μM quininib analogues on HMEC-1 endothelial cell migration. 50,000 cells were seeded and treated in duplicate for each individual experiment, and individual experiments were conducted three times ($n = 3$). *C*, effect of Q8 in combination with bevacizumab on HMEC-1 endothelial cell migration. 50,000 cells were seeded and treated in duplicate for each individual experiment, and individual experiments were conducted three times ($n = 3$). Migration was assessed using the xCELLigence system and RTCA software allowing real time monitoring of cell migration over 8 h. The real time traces (*B* and *C*, *right*) represent averaged data of all detected/bound cells from 0 to 8 h. Statistical analysis was performed by ANOVA, Dunnett's post hoc multiple comparison test, and Student's *t* test. *Error bars* are mean ± S.E. *, $p < 0.05$; **, $p < 0.01$; ***, $p < 0.001$; *ns*, not significant.

Q8 produced only a 22.9% antagonism of $CysLT_2$ receptor activation in HEK-293 cells. Thus, Q8 was excluded as a $CysLT_2$ antagonist as inhibition lower than 50% is considered insignificant. In relation to VEGF receptors, above threshold inhibition was only observed with VEGFR2 or VEGFR3 at higher concentrations. Using a cell-based ligand binding assay, 10 μM Q8 only inhibited ^{125}I-VEGF binding to VEGFR1 by 23%, well below the 50% inhibition cutoff regarded as significant (Eurofins Pharma

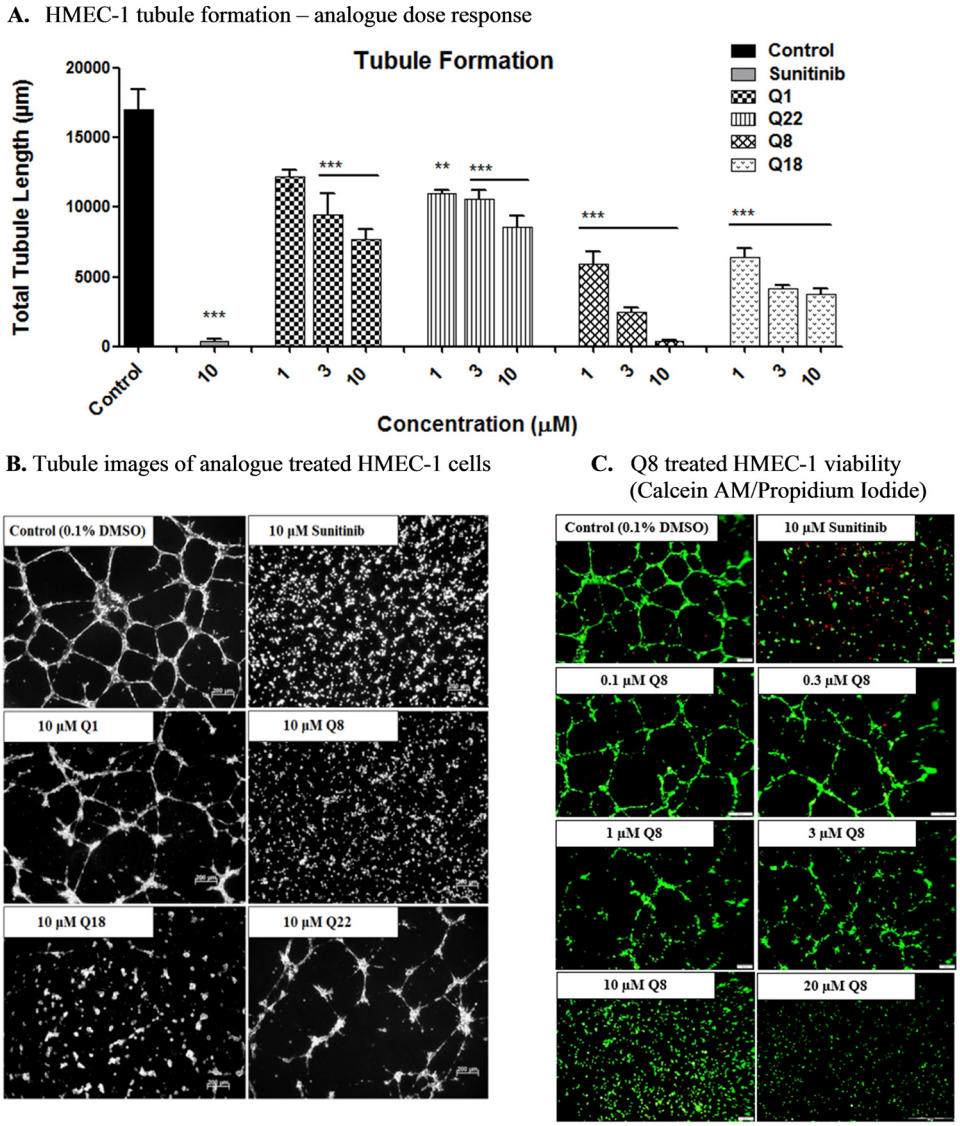

FIGURE 3. **Quininib analogues inhibit human endothelial cell tubule formation and do not affect HMEC-1 viability.** *A*, total tubule length following tubule formation of HMEC-1 endothelial cells treated with 1, 3, or 10 μM quininib analogues for 16 h. 7,500 cells were seeded in μ-Slide angiogenesis wells and treated in duplicate for each individual experiment, and individual experiments were conducted six times ($n = 6$). *B*, representative tubule images following treatment of HMEC-1 endothelial cells with 10 μM Q1 or analogues Q8, Q18, and Q22 for 16 h. *C*, viability images of Q8 (0.1–20 μM)-treated HMEC-1 endothelial cell tubules stained with calcein AM (*green*) and propidium iodide (*red*). 7,500 cells were seeded in μ-Slide angiogenesis wells and treated in duplicate for each individual experiment, and individual experiments were conducted three times ($n = 3$). Statistical analysis was performed by ANOVA and Dunnett's post hoc multiple comparison test. *Error bars* are mean ± S.E. **, $p < 0.01$; ***, $p < 0.001$.

Discovery Services). Similarly, 1 or 3 μM Q8 did not inhibit the kinase activity of VEGFR2 or VEGFR3, producing inhibitions (−34 to −24% or 29–46%, respectively) below the 50% threshold. However, 10 μM Q8 inhibited VEGFR2 kinase activity by 65% and VEGFR3 kinase activity by 78%.

We correlated the expression levels of $CysLT_1$ in Tg(*fli1*:EGFP) zebrafish larvae and in HMEC-1 endothelial cells during time points when quininib analogues induced antiangiogenic phenotypes (Fig. 6*B*). Levels of $CysLT_1$ gene expression were highest in 2-dpf Tg(*fli1*:EGFP) larvae (stage of intersegmental vessel growth analyses) compared with 6-hpf, 1-dpf, and 3-dpf larvae (Fig. 6*B*) The $CysLT_1$ receptor is traditionally associated with a cell membrane location; however, $CysLT_1$ also resides within the nuclear compartment (27). We demonstrate that the nuclear form of $CysLT_1$ is abundantly expressed in the HMEC-1 cells utilized for tubule formation and migration assays (Fig. 6*B*). We treated HMEC-1 endothelial cells for 5 h with 10 μM Q1, Q8, and the clinically used bronchodilator and anti-inflammatory $CysLT_1$ antagonist montelukast. Q8 reduced expression levels of the putative downstream $CysLT_1$ mediator calpain-2 by ~22% compared with control ($p = 0.0425$), but there was no significant change in levels of calpain-2 following treatment of HMEC-1 cells with Q1 or montelukast (Fig. 6*C*). Furthermore, we analyzed activated NF-κB p65 in HMEC-1 cell lysates and found that 10 μM Q8 reduced NF-κB levels by ~32% ($p < 0.001$) compared with control. In contrast, there were no significant changes in activated levels of NF-κB p65 following treatment with Q1 or montelukast (Fig. 6*D*). To determine whether levels of positive regulators of angiogenesis were altered by quininib analogues, secretions of Ang-1, Ang-2, bFGF, VEGF, ICAM-1, and VCAM-1 were quantified from HMEC-1 endothelial cells following treatment

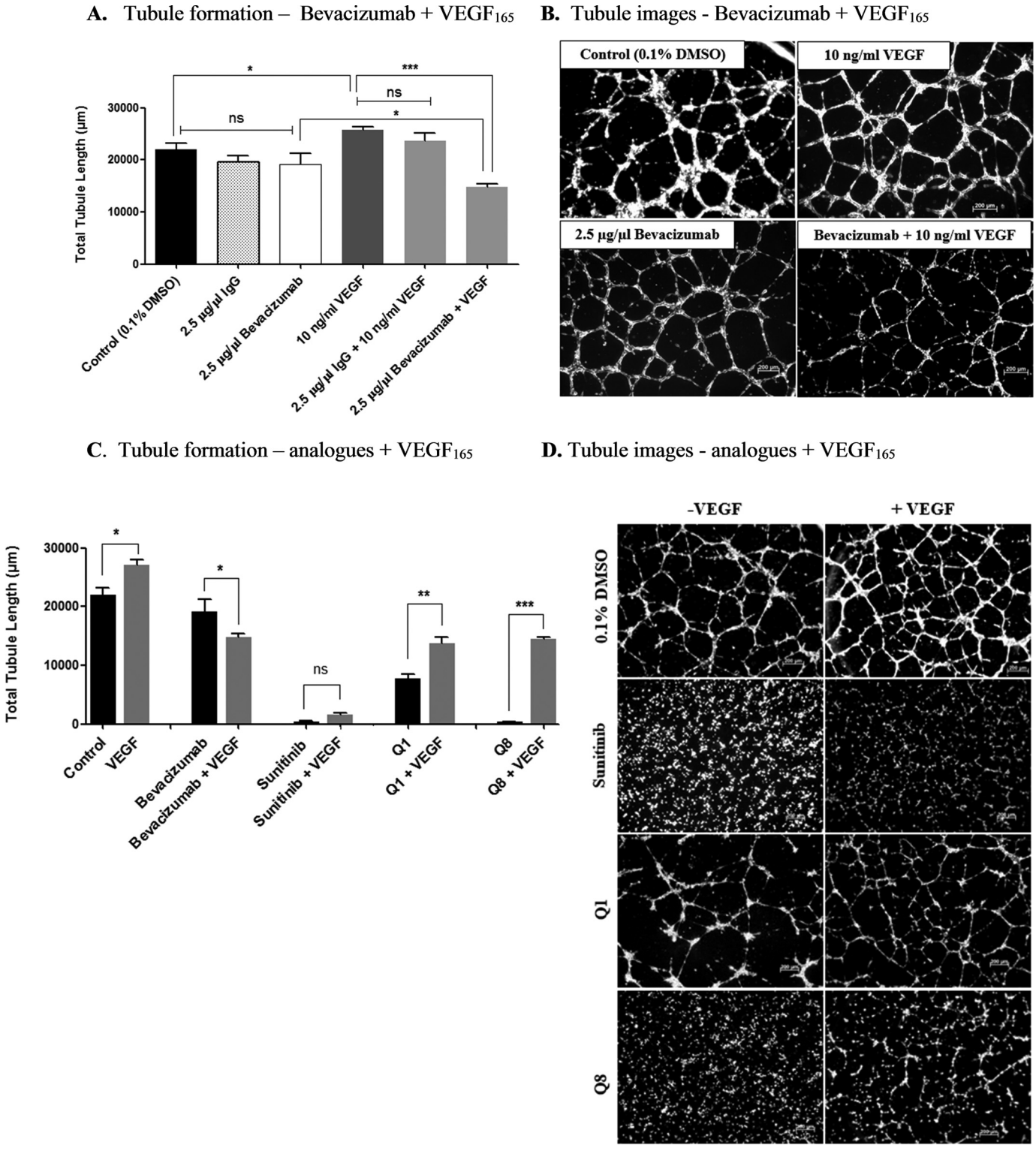

FIGURE 4. **Quininib analogues inhibit VEGF-independent angiogenesis *in vitro*.** *A*, HMEC-1 endothelial cell tubule formation is not affected following 16-h treatment with bevacizumab alone; however, when cells are treated with a combination of recombinant VEGF and bevacizumab, a significant reduction in tubule formation occurs following 16 h. 7,500 cells were seeded in μ-Slide angiogenesis wells and treated in duplicate for each individual experiment, and individual experiments were conducted three times ($n = 3$). *B*, representative tubule images of HMEC-1 cells treated with bevacizumab alone or in combination with recombinant VEGF. *C*, the effects of Q1 and analogue Q8 on HMEC-1 tubule formation are significantly diminished when cells are treated in combination with VEGF. 7,500 cells were seeded in μ-Slide angiogenesis wells and treated in duplicate for each individual experiment, and individual experiments were conducted three times ($n = 3$). *D*, tubule images of HMEC-1 cells treated with Q1 or analogue Q8 alone or in combination with VEGF. Statistical analysis was performed by ANOVA and Dunnett's or Bonferroni's post hoc multiple comparison test and Student's *t* test. *Error bars* are mean ± S.E. *, $p < 0.05$; **, $p < 0.01$; ***, $p < 0.001$; *ns*, not significant.

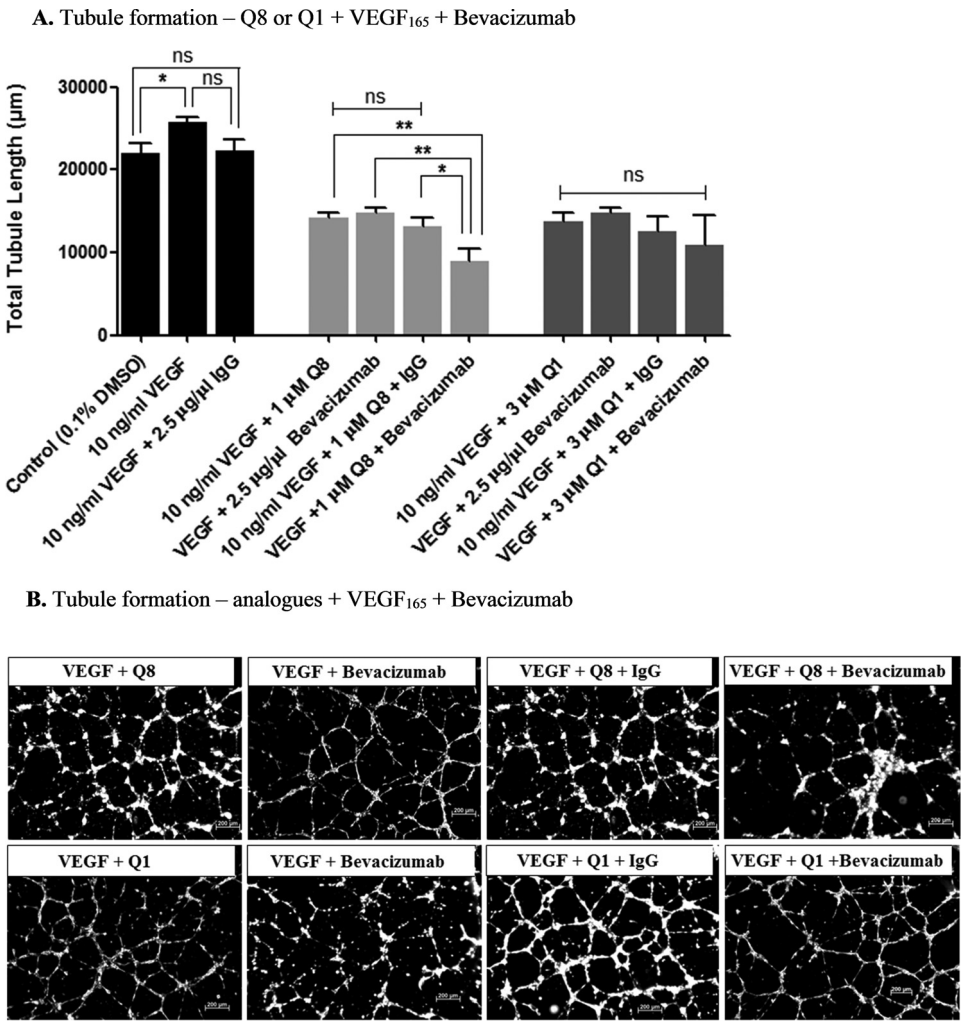

FIGURE 5. **Q8 has additive antiangiogenic effects with an anti-VEGF biologic, bevacizumab.** *A*, HMEC-1 endothelial cell tubule formation was significantly reduced following 16-h treatment with analogue Q8 in combination with bevacizumab compared with treatment with Q8 or bevacizumab alone. Q1 did not significantly reduce tubule formation in combination with bevacizumab compared with treatment with quininib or bevacizumab alone. 7,500 cells were seeded in μ-Slide angiogenesis wells and treated in duplicate for each individual experiment, and individual experiments were conducted three times ($n = 3$). *B*, representative tubule images of HMEC-1 endothelial cells treated with analogue Q8 or Q1 alone or in combination with bevacizumab for 16 h. Statistical analysis was performed by ANOVA and Dunnett's or Bonferroni's post hoc multiple comparison test and Student's *t* test. *Error bars* are mean ± S.E. *, $p < 0.05$; **, $p < 0.01$; *ns*, not significant.

with 10 μM quininib, Q8, Q22, Q18, and 2.5 μg/μl bevacizumab (Fig. 6*E*). Ang-1 secretion was reduced by quininib, Q8, and Q18 but not by the anti-VEGF bevacizumab. VEGF levels were significantly decreased by Q8 and bevacizumab only. Ang-2 secretion was reduced by all compounds including bevacizumab. Q8 was the only drug that significantly reduced the secretions of soluble VCAM-1 and ICAM-1 (Fig. 6*E*). The dual attenuation by bevacizumab and Q8 on VEGF levels together with the exclusive attenuation by Q8 on levels of ICAM-1 and VCAM-1 may explain the additive antiangiogenic effect observed with bevacizumab and Q8 in combination.

In summary, Q8 is a $CysLT_1$ antagonist with an IC_{50} of 4.9 μM. $CysLT_1$ is expressed in the zebrafish developmental stages and human endothelial cells in which quininib analogues exert antiangiogenic effects. Q8 significantly reduces endothelial cell secretion of the proangiogenic $CysLT_1$ downstream mediators VEGF, ICAM-1, VCAM-1, NF-κB, and calpain-2. Q8 can produce antiangiogenic effects independently of VEGF, supporting a distinct mechanism of action. Q8 also exerts an additive antiangiogenic response in combination with the anti-VEGF bevacizumab, likely due to some key proangiogenic factors being mutually reduced by both drug agents and others specifically reduced by bevacizumab or Q8.

Discussion

Organ growth and reparation rely on the growth of additional vasculature through angiogenesis. However, a disparity in the regulation of this process leads to various proangiogenic diseases including cancer, blindness, and rheumatism, and it is estimated that ~500,000,000 people will benefit from the development of antiangiogenic therapies over the next 20–30 years (3). The most recognized antiangiogenic therapies are the anti-VEGFs, particularly the anti-$VEGF_{165}$ recombinant humanized monoclonal antibody bevacizumab (Avastin) (3). Despite the promising effects that bevacizumab exhibited in animal models of tumor growth, it only extends life in colorectal cancer patients by ~4.7 months (17), in non-small cell lung cancer patients by ~13 months (18), and in cervical cancer

patients by ~17 months (31), and it failed to show any overall survival benefit in breast cancer patients (20). Given the evolving evidence that mediators other than VEGF promote the angiogenic switch in malignancy (32), the clinical potential for combining an anti-VEGF biologic with an inhibitor of a novel proangiogenic target is irrefutable (3). Such an approach could reduce clinical resistance to antiangiogenic therapy and increase treatment efficacy (33).

Phenotype-based screening of a library of small molecules led to the identification of the $CysLT_1$ antagonist quininib, a novel inhibitor of ocular and tumor angiogenesis (22, 23). Through structural modification of quininib, analogues that more effectively and potently inhibit intersegmental vessel formation in zebrafish larvae were developed. Indeed, the antiangiogenic effects of clinically tested agents such as SU5416 have been validated using zebrafish vasculature assays (34). Our

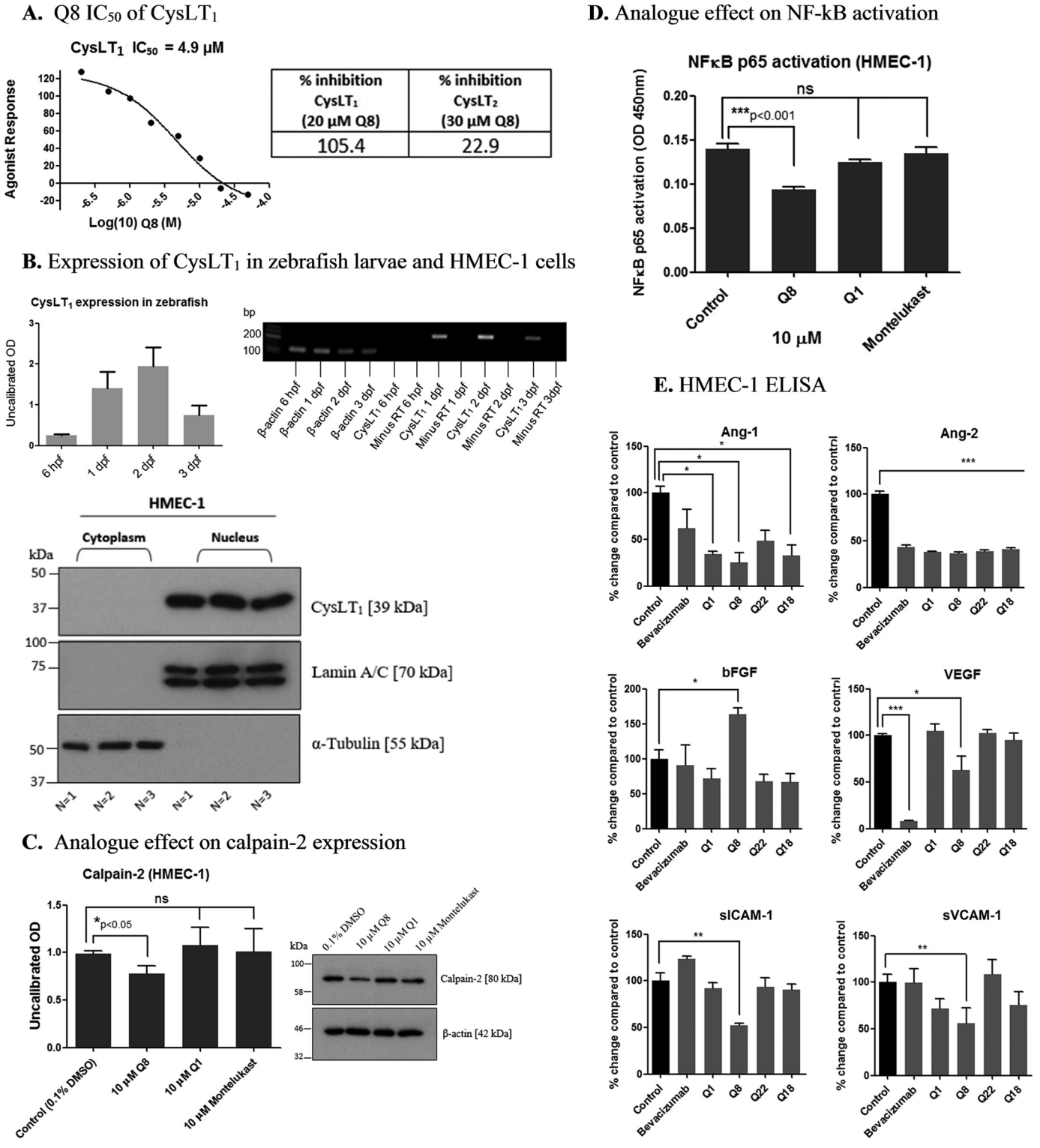

highest ranking antiangiogenic analogue from *in vivo* dose-dependent screening was Q8, also a $CysLT_1$ antagonist. Stimulation of $CysLT_1$ signaling by the endogenous ligand LTD_4 leads to activation of the downstream mediators phospholipase C, phosphoinositide 3-kinase (P13K), and protein kinase C-α (PKCα) (35). These mediators converge to promote angiogenic processes through activation of cell migration and motility, cell proliferation and survival, and increasing levels of secreted VEGF through activation of NF-κB (Fig. 7*A*). Thus, antagonism of $CysLT_1$ can inhibit these proangiogenic processes. The parent compound, quininib, was first chemically described as an antagonist of $CysLT_1$ by Zamboni *et al.* (36). The positional substitution of quininib by way of inclusion of a hydroxy group in the R_1 position of the phenyl ring and incorporation of an (*E*)-ethenyl linkage between the quinoline and the phenyl ring gave rise to optimal $CysLT_1$ binding (36). The enhanced potency of Q8 compared with quininib and other analogues is likely due to the additional phenyl ring hydroxy group in the R_4 position. A structure-activity relationship study (37) highlighted the importance of hydroxy group positioning for the biological activity of the antiestrogen drug tamoxifen, demonstrating that specific hydroxy positioning enabled correct configuration of the alkylaminoethane side chain of tamoxifen, facilitating binding to the estrogen receptor. It is suggested that the carboxylate groups of the endogenous $CysLT_1$ ligand LTD_4 are recognized by the hydrophilic (ionic) binding site of $CysLT_1$ (36), and it is probable that the additional R_4 hydroxy group of the Q8 aryl ring leads to enhanced interaction with $CysLT_1$ either through additional hydrogen bonding or through the more electron-rich aryl system through π-π interactions.

Emerging evidence highlights the functional importance of the leukotrienes acting via $CysLT_1$ during blood vessel growth (22, 38). LTC_4, LTD_4, and LTE_4 are lipids that induce inflammation by binding to and activating $CysLT_1$ and $CysLT_2$ and the less functionally studied GPR17 and GPR99 ($CysLT_3$) (26). Increased production of TNF-α and NF-κB following $CysLT_1$ activation leads to up-regulation of VEGF and matrix metalloproteinases, leading to enhanced endothelial cell proliferation, migration, and vascular tubule formation (25). Endothelial cell proliferation and inflammation are induced via $CysLT_2$/Rho kinase- and $CysLT_1$/ERK-dependent pathways (39), and indeed quininib is known to inhibit LTD_4-induced phosphorylation of ERK (22). Interestingly, treatment of murine aortic explants with the $CysLT_1$ antagonist montelukast blocks the growth of vascular sprouts; however, antagonism of $CysLT_2$ using BAY-cyslt2 did not prevent sprouting, suggesting that $CysLT_1$ signaling has a more significant proangiogenic role (38). There is also a significant reduction in the incidence of cancer among asthmatic patients treated with the $CysLT_1$ antagonist montelukast (40, 41). Given the apparent opposing biological role of these receptors, we demonstrate in this study that our most effective antiangiogenic analogue, Q8, is indeed an antagonist of $CysLT_1$ but not of $CysLT_2$, outlining the potential biological specificity of its effects. The formation of new blood vessels under developmental and pathological conditions is dependent on the ability of endothelial cells to migrate beyond the capillary basal lamina following its degradation, proliferate, and form capillary tubules with lumens to conduct the flow of blood (42). Here, we show the $CysLT_1$ antagonist Q8 significantly inhibits human endothelial cell proliferation and has the most prominent inhibitory effects on cell migration and tubule formation compared with all other analogues. The effects of Q8 are not associated with significant changes in endothelial cell viability, suggesting that the reduction in tubule formation and cell number following Q8 treatment is not due to endothelial cell death. The antiangiogenic effect of quininib analogues does not depend on the inhibition of endothelial cell proliferation.

Concentrations of 1–10 μM of all analogues tested significantly inhibit tubule formation at 16 h post-treatment compared with control; however, a 10 μM concentration of each analogue does not affect cell proliferation in the MTT assay at 24 h. These data taken together suggest that higher concentrations of analogues may exert their antiangiogenic effects by causing endothelial cell growth arrest, and lower concentrations may inhibit endothelial cell migration but have negligible influence on cell growth.

Pathological angiogenesis is associated with consistent up-regulation of many proangiogenic mediators including bFGF, Ang-1, Ang-2, VCAM-1, ICAM-1, and VEGF-A. VEGF-A induces endothelial cell proliferation, migration, and vessel permeability and is the most recognized driver of cancer-related vascular growth and vascular leakage in age-related macular degeneration (43). *In vitro* tubule formation (tubulogenesis), first described in 1980 (44), mimics the fundamental later

FIGURE 6. **Quininib analogue Q8 is a cysteinyl leukotriene receptor-1 antagonist that affects inflammatory and angiogenic signaling pathways.** *A*, the $CysLT_1$ receptor IC_{50} of analogue Q8 was determined to be 4.9 μM following testing in a cell-based $CysLT_1$ receptor antagonist assay in CHO cells (Eurofins Cerep SA). The assay measured calcium mobilization using fluor-3-loaded CHO cells overexpressing $CysLT_1$ and stimulated with the $CysLT_1$ receptor antagonist LTD_4. 20 μM Q8 inhibited $CysLT_1$ activation by 105.4%. In contrast, 30 μM Q8 produced only a 22.9% antagonism of $CysLT_2$ receptor activation in HEK-293 cells. Thus, Q8 was excluded as a tangible $CysLT_2$ antagonist as results showing an inhibition lower than 50% were not considered significant. Treatment of cells for individual experiments was carried out in duplicate, and each experiment was conducted 3 times ($n = 3$). *B*, $CysLT_1$ is present in our angiogenesis models shown by the presence of the $CysLT_1$ transcript in zebrafish larvae at 6 hpf, 1 dpf, 2 dpf, and 3 dpf following PCR and the presence of the nuclear form of the receptor in HMEC-1 endothelial cells by Western blotting. PCR was carried out using RNA isolated from larvae during three separate experiments ($n = 3$), and Western blotting was conducted three separate times using protein lysates from cells treated in duplicate during three separate experiments ($n = 3$). *C*, Western blot of HMEC-1 cells treated for 5 h with 0.1% DMSO or 10 μM Q1, Q8, and montelukast. Expression of calpain-2, a putative calcium-sensitive downstream target of $CysLT_1$ signaling and proangiogenic mediator, is reduced following treatment of endothelial cells with 10 μM Q8. Calpain-2 Western blotting was conducted on protein lysates from cells treated during three separate experiments ($n = 3$). *D*, the levels of activated NF-κB p65 were significantly reduced following treatment of HMEC-1 cells with 10 μM Q8 for 5 h, whereas treatment of cells with 10 μM Q1 or the clinically used $CysLT_1$ antagonist montelukast for 5 h had no effect on levels of activated NF-κB p65. NF-κB p65 ELISA was conducted using protein isolated from cells treated on three separate occasions in duplicate ($n = 3$). *E*, ELISA of HMEC-1 endothelial cell-conditioned medium following 16-h treatment of cells with 10 μM Q1, Q8, Q22, and Q18 revealing significant reductions in important proangiogenic mediators angiopoietin-2, VEGF, ICAM-1, and VCAM-1. Compared with other analogues of Q1, Q8, our highest ranking analogue, was the only compound to significantly reduce soluble ICAM-1 (*sICAM-1*), soluble VCAM-1 (*sVCAM-1*), and VEGF. Conditioned medium collected from three separate experiments was analyzed in duplicate by ELISA ($n = 3$). Statistical analysis was performed by ANOVA, Dunnett's post hoc multiple comparison test, and Student's *t* test. *Error bars* are mean ± S.E. *, $p < 0.05$; **, $p < 0.01$; ***, $p < 0.001$.

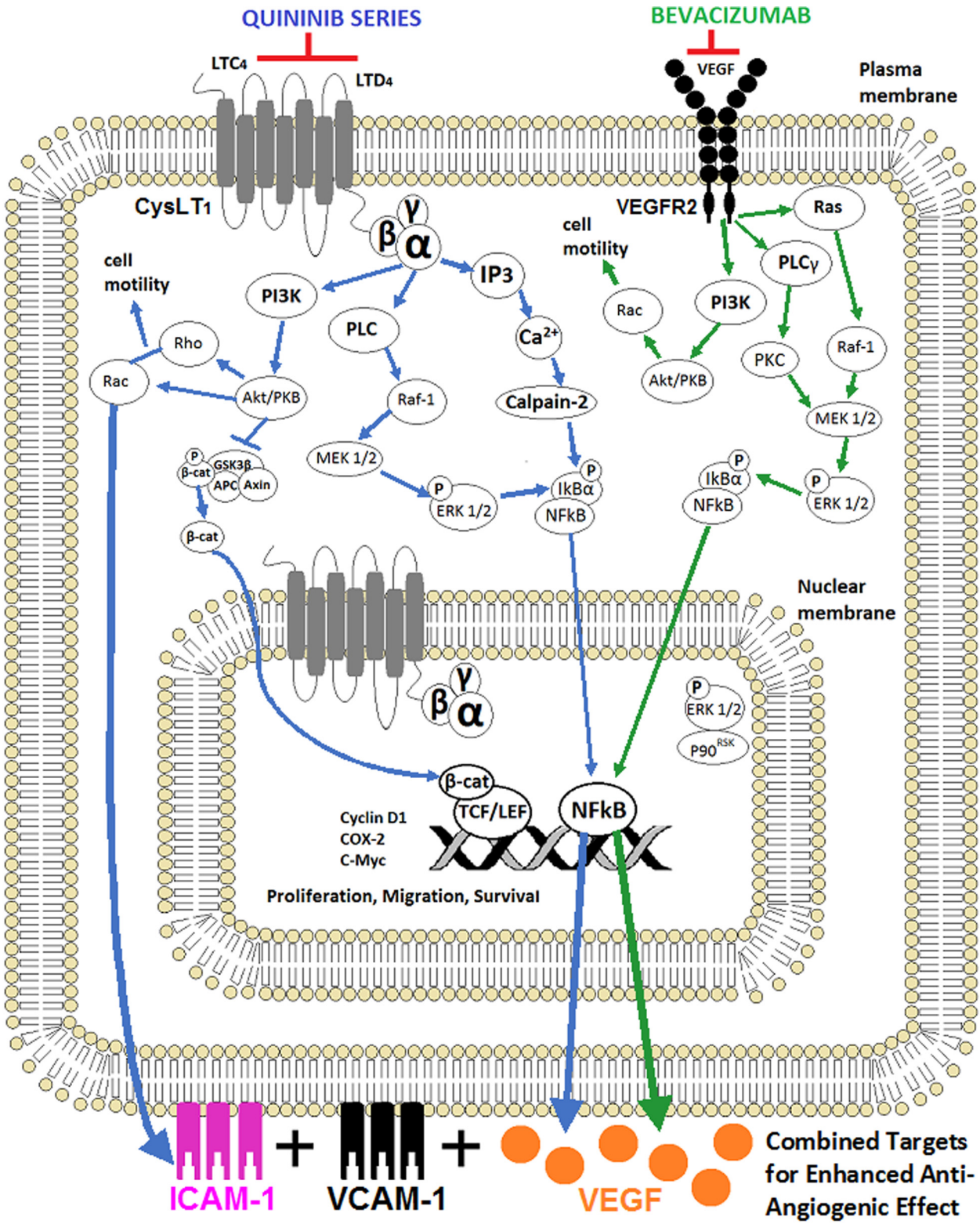

Drug	Pathway	ICAM-1% reduction	VCAM-1% reduction	VEGF % reduction
Q8	CysLT1 antagonist	48	44	37
Bevacizumab	anti-VEGF	0	0	92

stage processes of *in vivo* angiogenesis such as endothelial cell adhesion, migration, protease activity, and tubule formation (45) and can be significantly enhanced using the native ligand VEGF-A_{165} (42, 43, 46). Here, the *in vitro* tubule formation assay applied does not rely on VEGF-A as demonstrated by the ineffectiveness of bevacizumab to significantly reduce total tubule length in the absence of recombinant $VEGF_{165}$. The antiangiogenic activity of bevacizumab is only apparent in this tubule formation assay following co-administration with recombinant $VEGF_{165}$, a result similarly exemplified by Papadopoulos *et al.* (43) and Han *et al.* (46). In this manner, our quinoline compounds do not rely on the presence of VEGF to induce an antiangiogenic phenotype, suggestive of a novel mechanism of action. Furthermore, treatment of human endothelial cells with both quininib analogues and $VEGF_{165}$ reduces the antiangiogenic activity of the quininib analogues, which supports the hypothesis that these novel compounds do not directly inhibit VEGF. The absence of exogenous $VEGF_{165}$ in the combination migration assay (Fig. 2*C*) could explain the lack of effects on endothelial cell migration observed with bevacizumab and consequential lack of significant effects following treatment of cells with a combination of bevacizumab and Q8 compared with Q8 alone (Fig. 2*C*).

The effects of combining antiangiogenic treatments that have distinct mechanisms of action in cancer models is largely underinvestigated (3). We demonstrate for the first time that a combination of the anti-VEGF biologic bevacizumab and the novel $CysLT_1$ antagonist Q8 has enhanced additive antiangiogenic effects *in vitro* compared with treatment with either drug alone. Jia *et al.* (47) demonstrated an additive therapeutic effect where pancreatic tumor growth reduction and decreased tumor VEGF expression occurred following treatment of tumor-bearing mice with bevacizumab and the Sp1 inhibitor mithramycin A. This highlights the importance of this current study concerning the antiangiogenic additive effects of bevacizumab and Q8 *in vitro*. Moreover, two of the Q8 concentrations (1 and 3 μM) demonstrating a significant additive inhibitory effect on tubule formation in combination with bevacizumab show no significant inhibition of VEGFR1, VEGFR2, or VEGFR3. This supports a VEGF-independent action of this novel analogue at these concentrations. In cell-based ligand binding assays, inhibition of VEGFR1 with 10 μM Q8 was ~27%, well below the threshold regarded as significant. Also, in human KDR or FLT-4 kinase assays, 1 or 3 μM Q8 inhibited VEGFR2 and VEGFR3 below threshold levels. Interestingly, 10 μM Q8 inhibits VEGFR2 and VEGFR3 above the threshold regarded as significant. These data suggest a dual role for Q8 at higher concentrations wherein the compound may inhibit some VEGF receptors in addition to antagonizing $CysLT_1$. However, the relevance of these *in vitro* kinase results to the antiangiogenic activity in cell lines and *in vivo* has yet to be determined.

The evidence supporting the proangiogenic and protumorigenic role of leukotriene signaling has never been more ostensive (48). We show for the first time that Q8, a novel quinoline antagonist of $CysLT_1$, inhibits provascular phenotypes and reduces endothelial cell secretions of fundamental proangiogenic mediators including VEGF, ICAM-1, VCAM-1, NF-κB, and calpain-2. As the activity of the proangiogenic cysteine protease calpain-2 is calcium-dependent and $CysLT_1$ signaling activates inositol trisphosphate (49), we investigated whether the $CysLT_1$ antagonist Q8 would affect levels of this enzyme (50). Calpain-2 is a calcium-activated cysteine endopeptidase and a known regulator of VEGF-mediated angiogenesis (50). Calpain-2 facilitates IκBα degradation (51), enabling translocation of the VEGF inducer NF-κB to the nucleus. The association among calpain, NF-κB, and VEGF expression has been reported (52). In addition, an inhibitor of calpain reduces the levels of phospho-IκBα and inhibits release of proinflammatory mediators in mast cells (53). Western blotting analysis demonstrates that Q8 significantly reduces calpain-2 levels, and this enzyme has been reported to mediate IκBα degradation (51), enabling translocation of the VEGF inducer NF-κB to the nucleus. It is likely that antagonism of $CysLT_1$ by Q8 leads to decreased levels of secreted VEGF through inhibition of NF-κB (25, 54). Indeed, in the current study, we show that Q8 significantly reduces the activation of the NF-κB p65 unit compared with control. Prevention of angiogenesis through inhibition of NF-κB has long been a focus of anticancer therapy, and immense efforts have been made to develop specific NF-κB inhibitors (55–57).

The discernible reduction in levels of secreted ICAM-1 and VCAM-1 following treatment of HMEC-1 cells with Q8 may be a result of inhibition of Akt/PKB-induced Rho and Rac signaling (9, 11) following antagonism of $CysLT_1$. It is well understood that ICAM-1 and VCAM-1 signaling and function are regulated by the Rho-GTPases (10). Leukotriene signaling enhances the expression of ICAM-1 and VCAM-1 (25) where ICAM-1 is known to mediate endothelial progenitor cell recruitment (58) and VCAM-1 facilitates endothelial cell-cell interaction (59). VEGF has also been shown to mediate up-regulation of endothelial cell VCAM-1 and ICAM-1 through NF-κB activation (60). Q8 reduced secretions of ICAM-1 and VCAM-1 by ~48 and ~44%, respectively, but the parent compound Q1 only reduced the secretions of ICAM-1 and VCAM-1 by ~28 and ~8%, respectively. Analogue Q22 reduced secretions of ICAM-1 and VCAM-1 by ~0 and ~6%, respectively, and analogue Q18 reduced secretions of ICAM-1 and VCAM-1 by ~24 and ~9%, respectively. Ang-2 enables vascular destabilization and endothelial activation, enabling

FIGURE 7. **Proposed effects of combined targeting of $CysLT_1$ and VEGFR2 during angiogenesis.** Signaling schematic of $CysLT_1$ and VEGFR2. Following antagonism of $CysLT_1$, Q8 inhibits many of the instrumental processes that regulate angiogenesis such as cell motility, cytoskeletal reorganization, proliferation, and survival. Ca^{2+} influxes following Q8 antagonism are prevented, and the calcium-activated cysteine endopeptidase calpain-2 can no longer facilitate IκBα degradation. Hence, NF-κB is stabilized and will not translocate to the nucleus to induce expression of the angiogenic mediator VEGF. Additionally, antagonism of $CysLT_1$ by Q8, as demonstrated by ELISA, decreases the expression of ICAM-1 and VCAM-1, preventing endothelial cell motility and endothelial cell precursor recruitment. The enhanced additive antiangiogenic activity of Q8 is likely due to dual down-regulation of VEGF by Q8 and bevacizumab and the exclusive effects of Q8 on secreted levels of ICAM-1 and VCAM-1. *IP3*, inositol trisphosphate; *PLC*, phospholipase C; *APC*, adenomatous polyposis coli; *TCF*, T cell factor; *LEF*, lymphoid enhancer factor; *β-cat*, β-catenin. The table at the bottom of the figure denotes the percentage of decrease in secretion of ICAM-1, VCAM-1, and VEGF following treatment of human microvascular endothelial cells with either Q8 or bevacizumab, as determined by ELISA.

access of proangiogenic mediators to the endothelium. A reduction in Ang-2 may be the mechanistic output common to all of the quininib series of compounds as Ang-2 was the only angiogenic factor to be significantly down-regulated by all quininib drugs. However, Ang-2 was also down-regulated by bevacizumab, suggesting that regulation of other factors may be more important for the improved antiangiogenic effects of the higher ranking quininib analogue Q8. The survival of endothelial cells and the recruitment of pericytes are highly reliant on Ang-1 (61). Q1 and analogues Q8 and Q18 were the only compounds to significantly reduce endothelial cell secretion of Ang-1 by ~66, ~75, and ~67%, respectively. Q8 reduced endothelial cell secretions of VEGF by ~40%. Q1 and analogue Q22 failed to elicit any changes in secreted VEGF, and Q18 reduced VEGF secretion negligibly by ~4%. The additive antiangiogenic effects of Q8 in combination with the anti-VEGF bevacizumab may be clarified by the more significant effect of Q8 on levels of ICAM-1 and VCAM-1 in addition to the dual effect of Q8 and bevacizumab on levels of VEGF. A significant up-regulation of bFGF secretion was associated with Q8, possibly due to functional redundancy to compensate for lowered levels of VEGF (60, 62).

In conclusion, using an iterative phenotype-based ranking approach, we have developed structural analogues of quininib with novel and additive mechanisms of action, most notably analogue Q8, which has the most potent antiangiogenic activity *in vivo* and *in vitro* compared with all other analogues and is active in VEGF-independent models of angiogenesis. The dual effects of bevacizumab and Q8 on VEGF levels together with the exclusive effects of Q8 on levels of ICAM-1 and VCAM-1 may explain the additive antiangiogenic effect observed with bevacizumab and Q8 in combination. Novel small molecules such as the quininib series of compounds offer a novel therapeutic strategy to combat the inefficient clinical efficacy and resistance associated with conventional anti-VEGF therapies.

Experimental Procedures

Ethical Approval—Prior to commencing zebrafish ISV screens, the study was approved by the UCD Animal Research Ethics Committee under protocol number AREC-P-11-22.

Small Molecule Chemicals for in Vivo and in Vitro Experiments—Quininib analogues were synthesized by Celtic Catalysts (Ireland). Analogues were dissolved in 100% DMSO and diluted in embryo medium to test concentrations of 0.1–10 μM *in vivo* (final DMSO concentration was 0.1%). For *in vitro* experiments, 5-fluorouracil (Sigma F6627), montelukast (Selleckchem S4211), quininib, and its structural analogues Q22, Q8, and Q18 were dissolved in 100% DMSO as 10 mM stock solutions and stored at −20 °C. Working concentrations (0.1–10 μM) were prepared by dissolving stock solution in cell culture medium or H_2O, giving a final DMSO concentration of 0.1%.

Zebrafish (Danio rerio) Husbandry—Adult transgenic Tg(*fli1*:EGFP) zebrafish, which express enhanced green fluorescent protein (EGFP) in all endothelial cells, were kept on a 14-h light/10-h dark cycle at 28 °C. Male and female adult Tg(*fli1*:EGFP) zebrafish were in-crossed to produce embryos, which were subsequently staged using morphological assessment to obtain 6-hpf embryos (30).

Intersegmental Vessel Assay—During the primary screen, all compounds were tested at 10 μM. During dose-dependent screening, the parent compound Q1 and its analogues Q8, Q18, and Q22 were tested at 0.1–10 μM by incubating with five 6-hpf Tg(*fli1*:EGFP) embryos in 48-well plates for 48 h. At 2 dpf, the larvae were removed from their chorions and fixed in 4% paraformaldehyde, left for 2 h at room temperature, washed with PBS, and left at 4 °C before analysis using fluorescence microscopy.

Fluorescence Microscopy—An Olympus SZX16 stereo zoom microscope with an Olympus DP71 camera and cellSens software (Olympus) captured fluorescent and bright field images of fixed 2-dpf larvae. Intersegmental vessels were manually counted using high magnification, and fluorescent images of Tg(*fli1*:EGFP) larvae were obtained by EGFP excitation/emission filters (400 nm/509 nm).

Intersegmental Vessel Assay Scoring System for Efficacy, Potency, and Toxicity—To rank efficacy, compounds that inhibited intersegmental vessel growth in 2-dpf Tg(*fli1*:EGFP) larvae by 80–100% were allocated a score of 5, by 60–79% were allocated a score of 4, by 40–59% were allocated a score of 3, by 20–39% were allocated a score of 2, and by 1–19% were allocated a score of 1, and inhibition by 0% scored 0. To rank potency, compounds that could significantly inhibit ISV formation at 0.1 μM were allocated a score of 6, at 0.5 μM scored 5, at 1 μM scored 4, at 2.5 μM scored 3, at 5 μM scored 2, and only at 10 μM scored 1. Potency and efficacy scores contributed to a total ranking score for each compound. Following determination of the lowest concentration of each compound that significantly reduced intersegmental vessel growth, these data were compared with the degree of larval death. Compounds at the lowest effective concentrations that induced larval death by 80–100% were allocated a score of 0, by 60–79% were allocated a score of 1, by 40–59% were allocated a score of 2, by 20–39% were allocated a score of 3, and by 1–19% were allocated a score of 4, and if larval death was 0% these compounds scored 5.

Preparation of Clinical Drugs and Recombinant Protein for Cell-based Assays—Bevacizumab (Avastin) (Genentech) (25 mg/ml) was, unless otherwise stated, tested at 2.5 μg/μl. Recombinant $VEGF_{165}$ (R&D Systems 293-VE-010) was reconstituted from lyophilized form to 100 μg/ml using sterile PBS containing 0.1% bovine serum albumin and stored at −20 °C in 10-μl aliquots.

Cell Culture—HMEC-1 cell line was sourced from American Type Culture Collection (ATCC) and maintained at 37 °C at 5% CO_2 in MCDB-131 medium (Gibco 10372) supplemented with 10% FCS, L-glutamine (Gibco 25030-032), 1 μl/ml hydrocortisone (Sigma H0396), 10 ng/ml EGF (BD Biosciences 354001), and 1% penicillin-streptomycin (Gibco 151040-148).

MTT Assay—HMEC-1 cells were trypsinized using 2 ml of TrypLE™ Express (1×) (Invitrogen) and centrifuged at 1200 rpm for 4 min at room temperature. The cell pellet was resuspended in full medium, and cells were counted and seeded into 96-well plates at a density of 10,000 cells/well. Cells were left to adhere for 24 h and serum-starved for 24 h. Medium was removed and replaced with 10 μM drug. 5-Fluorouracil was

used as a positive control, and DMSO was used as the vehicle control. HMEC-1 cells were treated with 10 μM analogues for 24, 72, and 96 h. Drug solution was removed, and wells were washed with PBS before adding 10 μl of MTT dye to cells for 4 h at 37 °C. 100 μl of 100% DMSO was added to wells to dissolve the formazan crystals that formed. The absorbance values were read at 570 nm using a SpectraMax® M2 microplate reader.

Migration Assay—The migration of HMEC-1 human endothelial cells toward a 10% FBS medium solution was observed using a CIM plate 16 (RTCA DP Analyzer, xCELLigence). To prepare the CIM plate, medium containing chemoattractant or serum-free medium was pipetted into each lower well, and the upper chamber was clicked into position above these wells. 30 μl of serum-free medium was added to cover the surface of the microporous membrane, and the plate was incubated at 37 °C in 5% CO_2 for ≥1 h. After this time, a background reading of the plate with no cells was taken. HMEC-1 cells were trypsinized and resuspended in MCDB-131 medium with 10% FBS. 50,000 cells were seeded in duplicate and treated with 10 μM quininib, Q22, Q8, and Q18 analogues or with 0.1% DMSO control. Each CIM-16 plate well has a lower chamber containing 10% FBS as a chemoattractant and an upper chamber containing cells (±treatments) in serum-free medium. The chambers are separated by a microporous membrane with gold electrodes on the lower side. Cells bind to the gold electrodes when they migrate from the upper chamber through the membrane and cause an electrical impedance, which is recorded by an electric sensor plate and which correlates to the number of cells bound. HMEC-1 cells were treated with 2.5 μg/μl bevacizumab and either 1 or 3 μM Q8 for combination migration experiments. Cells were left to settle at room temperature for 30 min, and the CIM plate was placed into the RTCA DP Analyzer at 37 °C in 5% CO_2, and recording of the cell index occurred every 15 min. At the 8-h time point, the cell index values were analyzed and graphed using the RTCA software (Roche Applied Science).

In Vitro Tubule Formation Assay—The wells of a μ-Slide angiogenesis plate were coated with a layer of Matrigel matrix (BD Biosciences), which was left to form a gel for 45 min at 37 °C. HMEC-1 cells were grown to 80% confluence, washed with Dulbecco's PBS (Invitrogen) and trypsinized using TrypLE Express (1×). 7.5×10^3 cells were pipetted into each Matrigel-coated well of the μ-Slide angiogenesis plate and treated with either 0.1% DMSO; 1, 3, or 10 μM quininib or analogues Q22, Q8, and Q18; recombinant $VEGF_{165}$; or bevacizumab. The slide was kept at 37 °C in 5% CO_2 during tubule formations. After 16 h, the cells were imaged by phase-contrast microscopy using a Zeiss Axiovert 200M microscope. Total tubule length (μm) was quantified using Zeiss Axiovision image analysis software.

Calcein AM Staining—Calcein AM stain (Invitrogen C3099) was prepared at 2 μg/ml final concentration and incubated with HMEC-1 cells following tubule formation for 30 min at 37 °C. The stain was removed, cells were washed with PBS, and serum-supplemented cell medium was replaced. Cells were visualized and imaged under fluorescence microscopy using an Olympus SZX16 stereo zoom microscope with an Olympus DP71 camera and cellSens software.

Cysteinyl Leukotriene Receptor-1,2 Antagonism Assay—Q8 was assessed for antagonism of the cysteinyl leukotriene receptor 1 and cysteinyl leukotriene receptor 2 using cell-based (CHO and HEK-293) assays (22).

Vascular Endothelial Growth Factor Receptor Assays—For the ligand binding assay, the percentage of bound ^{125}I-VEGF in SF21 cells overexpressing human recombinant VEGFR1 was quantified by scintillation counting. Evaluation of the inhibitory effects of Q8 on the activity of human KDR kinase (VEGFR2) and human FLT-4 kinase (VEGFR3) were quantified by measuring the phosphorylation of the substrate Ulight-CAGAGAIETDKEYYTVKD (JAK1) using a human recombinant enzyme and the LANCE® detection method (Eurofins Cerep SA). Inhibition higher than 50% is considered significant.

Zebrafish Larval $CysLT_1$ Expression Analysis—RNA was isolated from larvae using TRIzol® (Invitrogen) according to the manufacturer's protocol. RNA samples were stored at −80 °C. Concentrations of RNA were obtained using spectrophotometry, and the quality of samples was deciphered using optical density (OD) measurements. RNA extracted from larvae was reversed transcribed to produce cDNA using the SuperScript® III First-Strand Synthesis System for RT-PCR according to the manufacturer's instructions. $CysLT_1$ forward primer [5′-GGCATCTTGCGCACTCTACT-3′] and $CysLT_1$ reverse primer [5′-GCAAAGCGTGATGACCACAG-3′] were used to generate PCR products, which were electrophoresed for 50 min at 110 V. Gels were visualized with a gel image analyzing system (UVP Products). Intensities of PCR product bands were normalized to β-actin (zebrafish *actb* forward primer [5′-CGAGCAGGAGATGGGAACC-3′] and zebrafish *actb* reverse primer [5′-CAACGGAAACGCTCATTGC-3′]), and sizes were verified by loading 5 μl of DNA HyperLadder™ 1 onto the gel.

HMEC-1 $CysLT_1$ and Downstream Protein Expression Analysis—HMEC-1 cells were seeded at 250,000 cells/well, and following adherence, cells were serum-starved for 24 h. To assess $CysLT_1$ expression, cytosolic and nuclear proteins were extracted from cells using Buffer A (10 mM HEPES, pH 8, 1.5 mM $MgCl_2$, 10 mM KCl, 200 mM sucrose, 0.5 mM DTT, 0.25% IGEPAL, and 1× protease inhibitor) and Buffer B (20 mM HEPES, pH 8, 420 mM NaCl, 0.2 mM EDTA, 1.5 mM $MgCl_2$, 0.5 mM DTT, 25% glycerol, and 1× protease inhibitor), respectively. Following treatment of HMEC-1 cells with 10 μM Q1, Q8, or montelukast for 5 h, total protein was extracted from cells using radioimmune precipitation assay lysis buffer supplemented with sodium fluoride (Sigma), β-glycerol phosphate (Sigma), protease inhibitor (Sigma), and phosphatase inhibitor (Sigma). Protein concentrations were determined using the BCA protein assay kit (Fisher). Expression of proteins of interest was determined by immunoblotting. 20 μg of protein was prepared in 5× sample buffer, separated by 12% SDS-PAGE, transferred to PVDF membranes (Millipore), and probed with primary antibodies ($CysLT_1$, Abcam (ab151484), 1:2000; lamin A/C, Cell Signaling Technology (2032), 1:1000; α-tubulin, Santa Cruz Biotechnology (sc-32293), 1:200; calpain-2, Aviva Systems Biology (OALA08938), 1:2000; and β-actin, Sigma (A5441), 1:5000). Membranes were subsequently probed with anti-rabbit horseradish peroxidase (HRP)-labeled secondary antibody (Cell Signaling Technology (7074), 1:2000) or anti-mouse HRP-labeled secondary antibody (Cell Signaling Tech-

nology (7076), 1:2000). Protein bands were visualized by chemiluminescence detection using Pierce ECL Western blotting substrate. Optical densitometry was used to quantitatively measure levels of expressed protein using ImageJ software.

Enzyme-linked Immunosorbent Assays—Following treatment of HMEC-1 cells for 16 h with 10 μM quininib analogues, secretion of VEGF, ICAM-1, VCAM-1, Ang-1, Ang-2, and bFGF was analyzed using multiplex ELISAs (Meso Scale Discovery) on cell-conditioned medium according to the manufacturer's instructions. Following treatment of HMEC-1 cells for 5 h with 10 μM quininib analogues, cell lysates were isolated using radioimmune precipitation assay lysis buffer supplemented with sodium fluoride, β-glycerol phosphate, protease inhibitor, and phosphatase inhibitor, and protein concentrations were determined using the BCA protein assay kit. 20 μg of cell lysates were analyzed for levels of activated NF-κB p65 using a TransAM® NF-κB p65 kit (Active Motif) according to the manufacturer's instructions.

Statistical Analysis—GraphPad Prism version 5 was used for statistical analysis. Differences between group means were determined using a one-way ANOVA with Dunnett's post hoc multiple comparison or Bonferroni's multiple comparison test and Student's *t* test.

Author Contributions—C. T. B. conducted dose-dependent screening of quininib analogues in zebrafish and proliferation, migration, viability, additive, and mechanistic experiments in HMEC-1 cells; analyzed experimental results; and wrote the paper. A. L. R. carried out initial screening of quininib analogues in the ISV assay and organized commercial assays (Eurofins Cerep SA). M. T. optimized the endothelial cell migration assay using HMEC-1 cells and assisted with analysis of results. P. J. G. proposed the enhanced potency of Q8 following examination of its chemical structure. E. T. D. and G. C. assisted with proteomics. B. N. K. devised the project and experiments, assisted with experimental analysis and interpretation of the results, and wrote the paper with C. T. B. J. O. assisted with experimental design and analysis and revised and edited the paper.

Acknowledgments—We thank Dr. Anne Costello for teaching us the in vitro tubule formation assay and providing the HMEC-1 cell line and the Education and Research Centre St. Vincent's University hospital for providing bevacizumab. We thank Dimitri Scholz and Kasia Welzel of the UCD Conway Institute Imaging Core Technology department for assisting with imaging of HMEC-1 tubules. We thank Kieran Wynne for help with proteomics and Lorraine Burke for assisting with calpain-2 Western blotting.

References

1. Otrock, Z. K., Mahfouz, R. A., Makarem, J. A., and Shamseddine, A. I. (2007) Understanding the biology of angiogenesis: review of the most important molecular mechanisms. *Blood Cells Mol. Dis.* **39,** 212–220
2. Carmeliet, P. (2003) Angiogenesis in health and disease. *Nat. Med.* **9,** 653–660
3. Carmeliet, P. (2005) Angiogenesis in life, disease and medicine. *Nature* **438,** 932–936
4. Riaz, M. K., Bal, S., and Wise-Draper, T. (2016) The impending financial healthcare burden and ethical dilemma of systemic therapy in metastatic cancer. *J. Surg. Oncol.* **114,** 323–328
5. World Health Organization (2012) *GLOBOCAN 2012—Estimated Cancer Incidence, Mortality and Prevalence Worldwide in 2012*, International Agency for Research on Cancer, Lyon, France
6. Carmeliet, P., and Jain, R. K. (2000) Angiogenesis in cancer and other diseases. *Nature* **407,** 249–257
7. Carmeliet, P. (2000) Mechanisms of angiogenesis and arteriogenesis. *Nat. Med.* **6,** 389–395
8. Papetti, M., and Herman, I. M. (2002) Mechanisms of normal and tumor-derived angiogenesis. *Am. J. Physiol. Cell Physiol.* **282,** C947–C970
9. van Wetering, S., van den Berk, N., van Buul, J. D., Mul, F. P., Lommerse, I., Mous, R., ten Klooster, J. P., Zwaginga, J. J., and Hordijk, P. L. (2003) VCAM-1-mediated Rac signaling controls endothelial cell-cell contacts and leukocyte transmigration. *Am. J. Physiol. Cell Physiol.* **285,** C343–C352
10. Cernuda-Morollón, E., and Ridley, A. J. (2006) Rho GTPases and leukocyte adhesion receptor expression and function in endothelial cells. *Circ. Res.* **98,** 757–767
11. Jung, C. H., Lee, W. J., Hwang, J. Y., Seol, S. M., Kim, Y. M., Lee, Y. L., Ahn, J. H., and Park, J. Y. (2012) The role of Rho/Rho-kinase pathway in the expression of ICAM-1 by linoleic acid in human aortic endothelial cells. *Inflammation* **35,** 1041–1048
12. Fojo, T., and Grady, C. (2009) How much is life worth: cetuximab, non-small cell lung cancer, and the $440 billion question. *J. Natl. Cancer Inst.* **101,** 1044–1048
13. Smith, T. J., and Hillner, B. E. (2011) Bending the cost curve in cancer care. *N. Engl. J. Med.* **364,** 2060–2065
14. Bach, P. B. (2009) Limits on medicare's ability to control rising spending on cancer drugs. *N. Engl. J. Med.* **360,** 626–633
15. Montero, A. J., Escobar, M., Lopes, G., Glück, S., and Vogel, C. (2012) Bevacizumab in the treatment of metastatic breast cancer: friend or foe? *Curr. Oncol. Rep.* **14,** 1–11
16. Gunther, J. B., and Altaweel, M. M. (2009) Bevacizumab (Avastin) for the treatment of ocular disease. *Surv. Ophthalmol.* **54,** 372–400
17. Hurwitz, H., Fehrenbacher, L., Novotny, W., Cartwright, T., Hainsworth, J., Heim, W., Berlin, J., Baron, A., Griffing, S., Holmgren, E., Ferrara, N., Fyfe, G., Rogers, B., Ross, R., and Kabbinavar, F. (2004) Bevacizumab plus irinotecan, fluorouracil, and leucovorin for metastatic colorectal cancer. *N. Engl. J. Med.* **350,** 2335–2342
18. Lynch, T. J., Jr., Spigel, D. R., Brahmer, J., Fischbach, N., Garst, J., Jahanzeb, M., Kumar, P., Vidaver, R. M., Wozniak, A. J., Fish, S., Flick, E. D., Leon, L., Hazard, S. J., and Kosty, M. P., and ARIES Study Investigators (2014) Safety and effectiveness of bevacizumab-containing treatment for non-small-cell lung cancer: final results of the ARIES observational cohort study. *J. Thorac. Oncol.* **9,** 1332–1339
19. Loges, S., Schmidt, T., and Carmeliet, P. (2010) Mechanisms of resistance to anti-angiogenic therapy and development of third-generation anti-angiogenic drug candidates. *Genes Cancer* **1,** 12–25
20. Kümler, I., Christiansen, O. G., and Nielsen, D. L. (2014) A systematic review of bevacizumab efficacy in breast cancer. *Cancer Treat. Rev.* **40,** 960–973
21. Kotz, J. (2012) Phenotypic screening, take two. *Science-Business eXchange* 10.1038/scibx.2012.380
22. Reynolds, A. L., Alvarez, Y., Sasore, T., Waghorne, N., Butler, C. T., Kilty, C., Smith, A. J., McVicar, C., Wong, V. H., Galvin, O., Merrigan, S., Osman, J., Grebnev, G., Sjölander, A., Stitt, A. W., *et al.* (2016) Phenotype-based discovery of 2-[(*E*)-2-(quinolin-2-yl)vinyl]phenol as a novel regulator of ocular angiogenesis. *J. Biol. Chem.* **291,** 7242–7255
23. Murphy, A. G., Casey, R., Maguire, A., Tosetto, M., Butler, C. T., Conroy, E., Reynolds, A. L., Sheahan, K., O'Donoghue, D., Gallagher, W. M., Fennelly, D., Kennedy, B. N., and O'Sullivan, J. (2016) Preclinical validation of the small molecule drug quininib as a novel therapeutic for colorectal cancer. *Sci. Rep.* **6,** 34523
24. Galvin, O., Srivastava, A., Carroll, O., Kulkarni, R., Dykes, S., Vickers, S., Dickinson, K., Reynolds, A. L., Kilty, C., Redmond, G., Jones, R., Cheetham, S., Pandit, A., and Kennedy, B. N. (2016) A sustained release formulation of novel quininib-hyaluronan microneedles inhibits angiogenesis and retinal vascular permeability *in vivo*. *J. Control. Release* **233,** 198–207
25. Behl, T., Kaur, I., and Kotwani, A. (2016) Role of leukotrienes in diabetic retinopathy. *Prostaglandins Other Lipid Mediators* **122,** 1–9

26. Kanaoka, Y., Maekawa, A., and Austen, K. F. (2013) Identification of GPR99 protein as a potential third cysteinyl leukotriene receptor with a preference for leukotriene E4 ligand. *J. Biol. Chem.* **288,** 10967–10972
27. Magnusson, C., Mezhybovska, M., Lörinc, E., Fernebro, E., Nilbert, M., and Sjölander, A. (2010) Low expression of CysLT1R and high expression of CysLT2R mediate good prognosis in colorectal cancer. *Eur. J. Cancer* **46,** 826–835
28. Turtay, M. G., Firat, C., Samdanci, E., Oguzturk, H., Erbatur, S., and Colak, C. (2010) Effects of montelukast on burn wound healing in a rat model. *Clin. Invest. Med.* **33,** E413–E421
29. Kennedy, B. N., Reynolds, A., Kilty, C., O'Sullivan, J., and Baxter, A. D. (January 23, 2014) *Anti-angiogenic Compounds*. Patent WO 2014012889 A1
30. Tran, T. C., Sneed, B., Haider, J., Blavo, D., White, A., Aiyejorun, T., Baranowski, T. C., Rubinstein, A. L., Doan, T. N., Dingledine, R., and Sandberg, E. M. (2007) Automated, quantitative screening assay for antiangiogenic compounds using transgenic zebrafish. *Cancer Res.* **67,** 11386–11392
31. Tewari, K. S., Sill, M. W., Long, H. J., 3rd, Penson, R. T., Huang, H., Ramondetta, L. M., Landrum, L. M., Oaknin, A., Reid, T. J., Leitao, M. M., Michael, H. E., and Monk, B. J. (2014) Improved survival with bevacizumab in advanced cervical cancer. *N. Engl. J. Med.* **370,** 734–743
32. Edelman, M. J., and Mao, L. (2013) Resistance to anti-angiogenic agents: a brief review of mechanisms and consequences. *Transl. Lung Cancer Res.* **2,** 304–307
33. Wang, Z., Dabrosin, C., Yin, X., Fuster, M. M., Arreola, A., Rathmell, W. K., Generali, D., Nagaraju, G. P., El-Rayes, B., Ribatti, D., Chen, Y. C., Honoki, K., Fujii, H., Georgakilas, A. G., Nowsheen, S., *et al.* (2015) Broad targeting of angiogenesis for cancer prevention and therapy. *Semin. Cancer Biol.* **35,** (suppl.) S224–S243
34. Serbedzija, G. N., Flynn, E., and Willett, C. E. (1999) Zebrafish angiogenesis: a new model for drug screening. *Angiogenesis* **3,** 353–359
35. Savari, S., Vinnakota, K., Zhang, Y., and Sjölander, A. (2014) Cysteinyl leukotrienes and their receptors: bridging inflammation and colorectal cancer. *World J. Gastroenterol.* **20,** 968–977
36. Zamboni, R., Belley, M., Champion, E., Charette, L., DeHaven, R., Frenette, R., Gauthier, J. Y., Jones, T. R., Leger, S., Masson, P., McFarlane, C. S., Metters, F., Pong, S. S., Piechuta, H., Rokach, J., *et al.* (1992) Development of a novel series of styrylquinoline compounds as high-affinity leukotriene D4 receptor antagonists: synthetic and structure-activity studies leading to the discovery of (+-)-3-[[[3-[2-(7-chloro-2-quinolinyl)-(E)-ethenyl]phenyl][[3-(dimethylamino)-3-oxopropyl]thio]methyl]thio] propionic acid. *J. Med. Chem.* **35,** 3832–3844
37. Murphy, C. S., Parker, C. J., McCague, R., and Jordan, V. C. (1991) Structure-activity relationships of nonisomerizable derivatives of tamoxifen: importance of hydroxyl group and side chain positioning for biological activity. *Mol. Pharmacol.* **39,** 421–428
38. Xu, L., Zhang, L., Liu, L., Fang, S., Lu, Y., Wei, E., and Zhang, W. (2010) Involvement of cysteinyl leukotriene receptors in angiogenesis in rat thoracic aortic rings. *Pharmazie* **65,** 750–754
39. Duah, E., Adapala, R. K., Al-Azzam, N., Kondeti, V., Gombedza, F., Thodeti, C. K., and Paruchuri, S. (2013) Cysteinyl leukotrienes regulate endothelial cell inflammatory and proliferative signals through CysLT2 and CysLT1 receptors. *Sci. Rep.* **3,** 3274
40. Ohd, J. F., Nielsen, C. K., Campbell, J., Landberg, G., Lofberg, H., and Sjolander, A. (2003) Expression of the leukotriene D4 receptor CysLT1, COX-2, and other cell survival factors in colorectal adenocarcinomas. *Gastroenterology* **124,** 57–70
41. Tsai, M.-J., Wu, P.-H., Sheu, C.-C., Hsu, Y.-L., Chang, W.-A., Hung, J.-Y., Yang, C.-J., Yang, Y.-H., Kuo, P.-L., and Huang, M.-S. (2016) Cysteinyl leukotriene receptor antagonists decrease cancer risk in asthma patients. *Sci. Rep.* **6,** 23979
42. Adair, T. H., and Montani, J.-P. (2010) Chapter 2, Angiogenesis Assays, in *Angiogenesis* Section 2.1, *In vitro* assays,, Morgan and Claypool Life Sciences, San Rafael, CA
43. Papadopoulos, N., Martin, J., Ruan, Q., Rafique, A., Rosconi, M. P., Shi, E., Pyles, E. A., Yancopoulos, G. D., Stahl, N., and Wiegand, S. J. (2012) Binding and neutralization of vascular endothelial growth factor (VEGF) and related ligands by VEGF Trap, ranibizumab and bevacizumab. *Angiogenesis* **15,** 171–185
44. Folkman, J., and Haudenschild, C. (1980) Angiogenesis by capillary endothelial cells in culture. *Trans. Ophthalmol. Soc. UK* **100,** 346–353
45. Arnaoutova, I., and Kleinman, H. K. (2010) *In vitro* angiogenesis: endothelial cell tube formation on gelled basement membrane extract. *Nat. Protoc.* **5,** 628–635
46. Han, Y. S., Lee, J. E., Jung, J. W., and Lee, J. S. (2009) Inhibitory effects of bevacizumab on angiogenesis and corneal neovascularization. *Graefes Arch. Clin. Exp. Ophthalmol.* **247,** 541–548
47. Jia, Z., Zhang, J., Wei, D., Wang, L., Yuan, P., Le, X., Li, Q., Yao, J., and Xie, K. (2007) Molecular basis of the synergistic antiangiogenic activity of bevacizumab and mithramycin A. *Cancer Res.* **67,** 4878–4885
48. Burke, L., Butler, C. T., Murphy, A., Moran, B., Gallagher, W. M., O'Sullivan, J., and Kennedy, B. N. (2016) Evaluation of cysteinyl leukotriene signaling as a therapeutic target for colorectal cancer. *Front. Cell Dev. Biol.* **4,** 103
49. Alswied, A., and Parekh, A. B. (2015) Ca^{2+} influx through store-operated calcium channels replenishes the functional phosphatidylinositol 4,5-bisphosphate pool used by cysteinyl leukotriene type I receptors. *J. Biol. Chem.* **290,** 29555–29566
50. Su, Y., Cui, Z., Li, Z., and Block, E. R. (2006) Calpain-2 regulation of VEGF-mediated angiogenesis. *FASEB J.* **20,** 1443–1451
51. Schaecher, K., Goust, J.-M., and Banik, N. L. (2004) The effects of calpain inhibition on IκBα degradation after activation of PBMCs: identification of the calpain cleavage sites. *Neurochem. Res.* **29,** 1443–1451
52. Spirina, L. V., Kondakova, I. V., Choynzonov, E. L., Chigevskaya, S. Y., Shishkin, D. A., and Kulbakin, D. Y. (2013) Expression of vascular endothelial growth factor and transcription factors HIF-1, NF-κB expression in squamous cell carcinoma of head and neck; association with proteasome and calpain activities. *J. Cancer Res. Clin. Oncol.* **139,** 625–633
53. Lin, T. J. (May 19, 2011) *Inhibition of Calpain Reduces Allergic Inflammation*. U. S. Patent 20110117106 A1
54. Xie, T. X., Xia, Z., Zhang, N., Gong, W., and Huang, S. (2010) Constitutive NF-κB activity regulates the expression of VEGF and IL-8 and tumor angiogenesis of human glioblastoma. *Oncol. Rep.* **23,** 725–732
55. Calzado, M. A., Bacher, S., and Schmitz, M. L. (2007) NF-κB inhibitors for the treatment of inflammatory diseases and cancer. *Curr. Med. Chem.* **14,** 367–376
56. Baud, V., and Karin, M. (2009) Is NF-κB a good target for cancer therapy? Hopes and pitfalls. *Nat. Rev. Drug Discov.* **8,** 33–40
57. Park, M. H., and Hong, J. T. (2016) Roles of NF-κB in cancer and inflammatory diseases and their therapeutic approaches. *Cells* **5,** E15
58. Wu, Y., Ip, J. E., Huang, J., Zhang, L., Matsushita, K., Liew, C. C., Pratt, R. E., and Dzau, V. J. (2006) Essential role of ICAM-1/CD18 in mediating EPC recruitment, angiogenesis, and repair to the infarcted myocardium. *Circ. Res.* **99,** 315–322
59. Salajegheh, A. (2016) *Angiogenesis in Health, Disease and Malignancy*, pp. 375–379, Springer International Publishing, Basel, Switzerland
60. Lieu, C., Heymach, J., Overman, M., Tran, H., and Kopetz, S. (2011) Beyond VEGF: inhibition of the fibroblast growth factor pathway and antiangiogenesis. *Clin. Cancer Res.* **17,** 6130–6139
61. Metheny-Barlow, L. J., and Li, L. Y. (2003) The enigmatic role of angiopoietin-1 in tumor angiogenesis. *Cell Res.* **13,** 309–317
62. Lieu, C. H., Tran, H., Jiang, Z. Q., Mao, M., Overman, M. J., Lin, E., Eng, C., Morris, J., Ellis, L., Heymach, J. V., and Kopetz, S. (2013) The association of alternate VEGF ligands with resistance to anti-VEGF therapy in metastatic colorectal cancer. *PLoS One* **8,** e77117